UCSF
UC San Francisco Previously Published Works

Title
Reevaluating the Substrate Specificity of the L-Type Amino Acid Transporter (LAT1)

Permalink
https://escholarship.org/uc/item/5rr3f8h3

Journal
Journal of Medicinal Chemistry, 61(16)

ISSN
0022-2623

Authors
Chien, Huan-Chieh
Colas, Claire
Finke, Karissa
et al.

Publication Date
2018-08-23

DOI
10.1021/acs.jmedchem.8b01007

Peer reviewed

eScholarship.org Powered by the California Digital Library
University of California

Author Manuscript
Author Manuscript
Author Manuscript
Author Manuscript

HHS Public Access
Author manuscript
J Med Chem. Author manuscript; available in PMC 2019 August 23.

Published in final edited form as:
J Med Chem. 2018 August 23; 61(16): 7358–7373. doi:10.1021/acs.jmedchem.8b01007.

Reevaluating the Substrate Specificity of the L-Type Amino Acid Transporter (LAT1)

Huan-Chieh Chien[#,†], **Claire Colas**[#,‡,⊥], **Karissa Finke**[#,§,#], **Seth Springer**[#,§,∇], **Laura Stoner**[#,§], **Arik A. Zur**[†,O], **Brooklynn Venteicher**[§], **Jerome Campbell**[§,♦], **Colton Hall**[§], **Andrew Flint**[§,¶], **Evan Augustyn**[§,+], **Christopher Hernandez**[§], **Nathan Heeren**[§,■], **Logan Hansen**[§], **Abby Anthony**[§], **Justine Bauer**[§], **Dimitrios Fotiadis**[‖], **Avner Schlessinger**[*,‡], **Kathleen M. Giacomini**[*,†], **Allen A. Thomas**[*,§]

[†]Department of Bioengineering and Therapeutic Sciences, University of California, San Francisco, San Francisco, California 94158, United States [‡]Department of Pharmacological Sciences, Icahn School of Medicine at Mount Sinai, New York, New York 10029, United States [§]Department of Chemistry, University of Nebraska at Kearney, Kearney, Nebraska 68849, United States [‖]Institute of Biochemistry and Molecular Medicine, and Swiss National Centre of Competence in Research (NCCR) TransCure, University of Bern, 3012 Bern, Switzerland

[#] These authors contributed equally to this work.

Abstract

The L-type amino acid transporter 1 (LAT1, SLC7A5) transports essential amino acids across the blood—brain barrier (BBB) and into cancer cells. To utilize LAT1 for drug delivery, potent amino acid promoieties are desired, as prodrugs must compete with millimolar concentrations of

[*]**Corresponding Authors** A.A.T: thomasaa@unk.edu., K.M.G.: Kathy.Giacomini@ucsf.edu., A.S.: avner.schlessinger@mssm.edu. Phone, 308–455-0544.
[⊥]**Present Addresses** C.C.: Pharmacoinformatics Research Group, Department of Pharmaceutical Chemistry, University of Vienna, Althanstraße 14 (UZA II), 1090 Vienna, Austria.
[#]K.F.: 1500 Kansas University Clinical Research Center, 4350 Shawnee Mission Parkway, Fairway, Kansas 66205, United States.
[∇]S.S.: University of Nebraska Medical Center, Department of Pharmacology and Experimental Neuroscience, 985800 Nebraska Medical Center, Omaha, Nebraska 68198-5800, United States.
[O]A.Z.: BioLineRx Ltd., Modi'in Technology Park, 2 HaMa'ayan Street, Modi'in 7177871, Israel.
[♦]J.C.: Department of Chemical and Biological Engineering McCormick School of Engineering and Applied Science, Northwestern University, 2145 Sheridan Road, Room E-136, Evanston, Illinois 60208, United States.
[¶]A.F.: University of Nebraska Medical Center, College of Pharmacy, 986120 Nebraska Medical Center, Omaha, NE 68198-6120, United States.
[+]E.A.: Creighton University, School of Dentistry, 2500 California Plaza, Omaha, Nebraska 68178, United States.
[■]N.H.: University of Wyoming, School of Pharmacy, Health Sciences, Room 292, 1000 East University Avenue, Department 3375, Laramie, Wyoming 82071, United States.

ASSOCIATED CONTENT

Supporting Information

The Supporting Information is available free of charge on the ACS Publications website at DOI: 10.1021/acs.jmed-chem.8b01007.
Comparison of the homology model of LAT1 with AdiC in the outward occluded conformation, a table with binding site descriptions of templates and models in outward-occluded and outward-open conformations, model refinement and ligand docking description, optical rotation alongside comparison to literature values and LC-MS analysis of all purchased, tested amino acids, isolated yields for all Negishi coupling reactions, full compound characterization data and procedures, LC-MS traces and $^{1}H/^{13}C$ NMR spectra for key target compounds **74**, **79**, **81**, **82**, **83**, **86**, and **87**, a plot showing relative uptake of [^{3}H]-gabapentin into different cell types (PDF)
Molecular formula strings with LAT1 cell assay data for exemplified compounds (CSV)
LAT1 occluded homology model (PDB)
LAT1 open homology model (PDB)

The authors declare no competing financial interest.

Author Manuscript Author Manuscript Author Manuscript Author Manuscript

endogenous amino acids. To better understand ligand—transporter interactions that could improve potency, we developed structural LAT1 models to guide the design of substituted analogues of phenylalanine and histidine. Furthermore, we evaluated the structure—activity relationship (SAR) for both enantiomers of naturally occurring LAT1 substrates. Analogues were tested in cis-inhibition and *trans*-stimulation cell assays to determine potency and uptake rate. Surprisingly, LAT1 can transport amino acid-like substrates with wide-ranging polarities including those containing ionizable substituents. Additionally, the rate of LAT1 transport was generally nonstereoselective even though enantiomers likely exhibit different binding modes. Our findings have broad implications to the development of new treatments for brain disorders and cancer.

Graphical Abstract

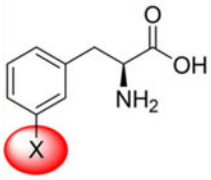

Compd	X	Relative exchange efflux rate (%)	LAT1 IC_{50} (μM)
50 (L-Phe)	H	100	69
74	$-CH_2NH_2$	78	470
81	$-CO_2{}^tBu$	70	17
82	$-CO_2(CH_2)_2OH$	74	29
83	$-CO_2H$	56	130

INTRODUCTION

The L-type amino acid transporter 1 (LAT1; SLC7A5), commonly referred to as the "large neutral amino acid transporter 1," is primarily expressed in brain, spleen, testis, placenta, thymus, skeletal muscle, and various cancer cells.[1–11] LAT1 exists as a heterodimeric complex of 12 putative membrane-spanning helices (light chain) with a glycoprotein 4F2hc (SLC3A2; heavy chain) and is responsible for importing lipophilic, neutral amino acids: leucine, isoleucine, valine, phenylalanine, tyrosine, tryptophan, methionine, and histidine.[12] Several amino acid-like drugs, including the Parkinson's drug L-DOPA[13,14] and gabapentin,[15,16] are transported across the blood—brain barrier (BBB) by LAT1. The transporter is expressed at 100-fold greater levels in the endothelial cells of the BBB than in other tissues.[2,17] For this reason, it has been a target of interest for delivering drugs into the brain via active transport.[18–24] Lately, there has been increasing attention given to its role in cancer,[25–27] in which LAT1 is upregulated in various tumors, to meet the increased nutritional needs of growing and proliferating tumor cells.[25–28] Additionally, LAT1 expression has been correlated with tumor aggressiveness and poor prognosis.[29–34] Furthermore, LAT1 inhibitors are successful at reducing cancer cell growth both in vitro and in vivo.[25,35–41]

LAT1 has been shown to transport amino acid-containing prodrugs, in which amino acids were linked with drug molecules.[18–24,41,42] Surprisingly, larger entities, including nanoparticles and liposomes, may be targeted to cell membranes by attachment of amino acids, presumably through interaction with LAT1.[43–46] Although it is not the only transporter that has been comprehensively investigated for drug delivery,[6,47–49] LAT1 is particularly suitable because it possesses a large maximal transport capacity (V_{max}),

Author Manuscript Author Manuscript Author Manuscript Author Manuscript

allowing many substrate molecules to pass per unit time. It also has a relatively low K_m for many of its substrates (e.g., K_m =11 μM for phenylalanine[50]), allowing such molecules to be transported at relatively low concentrations. Moreover, it is known that LAT1 tolerates various chemical modifications to the amino acid substrates that it recognizes.[4,51] Thus, amino acid-like drugs or prodrugs have the potential for a broad range of applications in treating CNS disorders and cancer.

One of the challenges for using LAT1 as a delivery tool has been the competition of the transported drugs with endogenous amino acids substrates, which have millimolar concentrations in the plasma.[50,52] For example, it has been shown that brain uptake of L-DOPA decreases after a meal rich in large amino acids,[53] and L-DOPA decreases the concentration of other amino acids (i.e., tyrosine and tryptophan) in the rat brain.[54] Potential antagonism by endogenous amino acids has been cited as a limitation for using this transporter in drug delivery.[55] One possible way to overcome this problem is by increasing the affinity of drugs or prodrugs for the transporter relative to natural amino acid substrates (K_m = 11–210 μM).[50] To date, there has been some progress in developing LAT1 substrate SAR by us[56–58] and others.[26,51,59] For example, it is known that substitution on the aromatic ring of phenylalanine derivatives, specifically at the meta position, is tolerated and can allow for improved brain uptake of prodrugs.[60] In addition, it has been reported that LAT1 demonstrates modest stereoselectivity for some of its substrates (i.e., Phe, Leu, and Met), while allegedly having greater stereoselectivity for others (i.e., Ile, Tyr, His, Trp, Val).[61] Furthermore, it has been shown that some d amino acids are taken into tumors via LAT1,[62] although it is presently unclear what physiological purpose there might be for LAT1 to transport D amino acids.

Despite these observations on LAT1 substrate SAR, several relevant and potentially misleading assumptions about the transporter have recurrently been stated in the literature:

1. Both the amino acid and carboxylic acid functional groups are essential for transporter recognition.[4,17,47]
2. Large, neutral side groups are required for ligand binding.[25,40,63–65]
3. LAT1 is mostly stereoselective for l amino acids.[1,66–68]

Recently, our team[57] and Nagamori[26] have shown that carboxylic ester and hydroxamic acid derivatives of several amino acids are most likely LAT1 substrates based on their ability to cause efflux of an intracellular radiolabeled substrate (e.g., [^{3}H]-gabapentin) via LAT1's alternating access transport mechanism (*trans*-stimulation cell assay).[57,58] Given this evidence that assumption 1 is incorrect, we wanted to determine whether assumptions 2 and 3 about substrate specificity might also be flawed.

Accordingly, the goal of our study was to increase our understanding of structure-activity relationships of LAT1 substrates, principally focused on the questions of whether neutral amino acids are required for substrate specificity and whether LAT1 translocates its substrates in a stereoselective fashion. As part of our ongoing effort to identify potent LAT1 ligands that expand LAT1 chemical space to non-natural amino acids that could potentially be used to design prodrugs for targeted drug delivery and/or antitumor agents,[56,57] we took

Author Manuscript Author Manuscript Author Manuscript Author Manuscript

an integrated approach that includes structural modeling of LAT1 binding to putative substrates and inhibitors, combined with testing of these compounds in cell assays. On the basis of the experimental results, models were refined. While the structure of the human LAT1 is not known, homology models developed by us[56–58] and others[69] have shown that LAT1 is a member of the large amino acids, polyamines, and organocations (APC) superfamily of transporters, which adopts a LeuT-like fold and uses a gated-pore alternating access transport mechanism.[70] Previous models of an outward-occluded conformation were used to guide SAR studies for this protein, but for the current work we developed a new outward-open model based on a recently solved structure of AdiC bound to agmatine.[71]

RESULTS AND DISCUSSION

Rational ligand design.

We have previously built homology models of the LAT1 light chain based on prokaryotic structures of the L-arginine/agmatine transporter AdiC in the outward-occluded facing conformation.[56–58] The LAT1 models based on AdiC were shown to be useful for rational design of novel LAT1 ligands.[41,56,58] For example, computational modeling and experimental testing of newly synthesized compounds guided the discovery of novel inhibitors and substrates consisting of carboxylate bioisosteres.[57] Both LAT1 and AdiC have a conserved structural fold and substrate specificity (amino acids) in addition to a highly similar binding site.[58,70] In particular, the binding site residues interacting with the amine and carboxylic acid groups of substrates are conserved between LAT1 and AdiC (Supporting Information, Figure S1). Conversely, the residues interacting with substrate side chains are more variable, contributing to the distinct specificities between LAT1 and AdiC.[72] Binding site differences such as Gly 255 (Ile 205 in AdiC) and Ser 342 (Trp 293 in AdiC) result in a larger accessible surface area in LAT1 (Supporting Information, Figure S1) and reveal unique subpockets termed pockets A, B, and C (Figure 1). Furthermore, previous studies have highlighted the residues involved in substrate binding using site-directed mutagenesis.[69] For example, mutations of Ser 342 and Cys 335 (Trp 293 and Cys 286 in AdiC) to Gly and Ala, respectively, resulted in decreased substrate activity. We hypothesized that targeting these regions of the binding site would allow us to discover compounds specific to LAT1 and with a higher affinity.

Recently, the AdiC structure was solved at high-resolution in a unique outward-open conformation with bound substrate, providing an excellent template for modeling LAT1 in this conformation (PDB 5J4N[71]). On the basis of this unique structure of AdiC, we generated a LAT1 model in the outward-open conformation (Experimental Section) to better inform ligand design. In brief, LAT1 consists of 12 transmembrane helices with a LeuT-like fold architecture, comparable to other APC family members (Figure 1a). The outward-occluded and outward-open models are generally similar (rmsd of 2.4 Å), exhibiting movements commonly observed in transporters utilizing the gated-pore mechanism. The most noticeable conformational change occurs in transmembrane helix 6 (TM6), which tilts away from the binding site in the outward-open conformation (Figure 1b). Interestingly, TM6 residue Phe252 faces alternatively inward or outward, closing or opening the binding site, thereby acting as a gate (Figure 1b,c). This gate is conserved in the AdiC structure

Author Manuscript Author Manuscript Author Manuscript Author Manuscript

where it is defined by Trp202[71] and has been shown to be essential for binding.[69] Consequently, the size and shape of the binding site is increased (Figure 1d and Supporting Information, Figure S1 and Table S1). This new conformation of LAT1 highlights the flexibility of its binding site and provides hypotheses regarding its transport mechanism and explanation for the activity of LAT1 ligands in the current work.

Guided by our new, outward-open model, we have investigated the SAR at various positions on the endogenous substrates phenylalanine and histidine as well as examined ligand stereoselectivity (Tables 1–3). We chose phenylalanine as a template for most of our SAR exploration due mainly to the synthetic convenience of substitution on its aromatic ring but also because of its relatively high affinity for the transporter.[61] We pursued modification of the phenylalanine scaffold chiefly at two positions: the aromatic meta position (Table 1) and the α position (Table 2). It has previously been shown by us and others that substitution at the meta position can provide enhanced substrate activity relative to the ortho and para positions.[56,60] Consistent with these results, our previously published LAT1 homology model in the outward-occluded conformation showed that the binding site could accommodate large substituents at the meta position in the subpocket termed pocket A (PA).[56] Furthermore, our model predicted the possibility for ligands to hydrogen bond with residues in PA (Figure 1c). Thus, we sought to determine whether we could improve potency and/or uptake rate by meta substitution with various polar functional groups capable of hydrogen bonding (Table 1). It has also been shown that methyl substitution at the α position of phenylalanine is tolerated.[73] Thus, we were curious as to whether larger groups at the α position (Table 2) might improve substrate activity through lipophilic interactions with the hydrophobic pocket C (PC, Figure 1c), proposed by our models. In addition to modification at these two positions, we prepared both enantiomers of selected phenylalanine analogues (i.e., compounds **79, 83**, and **110**, Table 1) and tested both enantiomers of various endogenous LAT1 substrates (Table 3). Although it had previously been reported that LAT1 was mostly stereoselective,[61] we were interested to determine how d isomers would perform in our cell assays, particularly in our *trans*-stimulation assay.

Cell-Based Assays.

To evaluate compounds' activities, both cis-inhibition and *trans*-stimulation assays using HEK cells engineered to overexpress human LAT1 were employed (Experimental Section).[58,74] The cis-inhibition assay allows for evaluation of LAT1 ligand binding, with IC_{50} value determinations providing a measure of binding potency relative to a radiolabeled substrate, [^{3}H]-gabapentin. In some cases, IC_{50} values which are determined by varying a test compound's concentration, did not track with what would have been expected from %inhibition data (e.g., compound **71**), as the latter is determined from only a single concentration of test compound. Though this *cis*-inhibition assay is beneficial for rank ordering compounds based on the strength of their interaction with the transporter, it cannot distinguish between substrates and inhibitors. Thus, to more directly identify substrates, we performed a *trans*-stimulation experiment[75] which exploits LAT1's exchanger activity[16,76] by loading cells with a radiolabeled substrate followed by incubation with extracellular test compound. The exchange efflux rate of the radiolabel in the presence of a test compound is compared with the efflux rate in the absence of the test compound as well as with

Author Manuscript Author Manuscript Author Manuscript Author Manuscript

nonsubstrates (e.g., L-arginine, **54**). Compounds that are LAT1 substrates should increase the efflux rate of the radiolabeled amino acid compared with its efflux rate in the absence of test compound or compared with the efflux rate observed in the presence of non-LAT1 substrates (e.g., L-arginine, **54**, Table 1). We selected [^{3}H]-gabapentin as a probe substrate due to its selectivity for LAT1 relative to other membrane transporters.[16] Two known LAT1 substrates (L-leucine and L-phenylalanine) and two nonsubstrates (L-glycine and L-arginine) served as positive and negative controls, respectively. The range of efflux rates we have observed in our assay is generally between 0.4 and 4.0 fmol/min, with nonsubstrates typically exhibiting an efflux rate of 0.4–0.8 due to background levels of exported [^{3}H]-gabapentin (Tables 1–3). This background efflux may be due to the presence of low concentrations of endogenous amino acids present in the cell assay media and/or resulting from export via an alternate transporter. To enable more facile comparisons between compounds' efflux rates, we have normalized efflux rates for all tested compounds (Tables 1–3) to the efflux rate of l-phenylalanine **50** (2.7 fmol/min, averaged from seven different experiments). Although *trans*-stimulation assays are widely used, the assay provides indirect evidence of whether a compound is a potential substrate of LAT1.[58] LC-MS or radiolabeled compound uptake experiments are still required for transporter kinetic parameters (i.e., K_m and V_{max}).[77] Additional discussion of the *trans*-stimulation assay has previously been published.[75,78,79]

SAR Discussion.

Compounds in Tables 1–3 were tested as ligands of LAT1 in both *cis*-inhibition and *trans*-stimulation assays as described above (more details provided in the Experimental Section).[56–58] From our previous work with phenylalanine derivatives[56] and in agreement with SAR published by others,[4,51] we found that aromatic substitution with hydrophobic groups (e.g., tert-butyl, benzyl, and phenyl as present in **68–70**, respectively) at the meta position provided increased LAT1 affinity but with concomitant loss in substrate activity, evidenced by the fact that these amino acids showed diminished efflux rates in our *trans*-stimulation cell assay. However, we cannot rule out the possibility that these compounds may simply have a slower transport rate than can be detected using our assay. On the basis of these observations, we hypothesized that substitution with polar functional groups at the meta position might allow for interactions with the transporter to improve ligand binding without losing substrate activity. Moreover, from our models, it appeared that there were multiple residues (e.g., Figure 1c: Ser143, Ser338, and Asn404) near the meta position that might be capable of dipole–dipole or hydrogen bonding interactions with polar substituents that could result in greater transporter affinity. To test these ideas, we substituted phenylalanine's aromatic ring at both the meta and para positions with various polar functional groups (Table 1), selected for diversity in forming hydrogen bonds at different angles and having a range of cLogP and tPSA values (Figure 2).

Remarkably, the meta position of phenylalanine is considerably more tolerant of substituents with vastly different polarities than could have been predicted based on previously published models of the binding site.[4,59] Although we observed little correlation between cLogP and tPSA with a substrate's affinity for the transporter (Figure 2), the more hydrophobic amino acids possessing positive cLogP values (i.e., **69** and **70**) were the most potent ligands, with

Author Manuscript Author Manuscript Author Manuscript Author Manuscript

diminished efflux rates compared with L-phenylalanine **50**. Furthermore, it is unclear from the current SAR whether there is an optimum distance away from the aromatic ring for a hydrogen bond acceptor as a previous model had proposed.[59] For example, amides 75 and 76 have identical activity within the error of our assays. Upon observing that a meta methyl ester substituent in 79 gave a modest improvement in IC_{50} relative to parent phenylalanine (IC_{50}s 36 vs 69 μM, respectively), we were prompted to follow up with additional esters at this position and at the para position. Unexpectedly, both a bulky, hydrophobic *tert*-butyl group in 81 and a polar, hydroxyethyl substituent in 82 provided the most potent substrates in the current work, with comparable IC_{50} values of 17 and 29 μM, respectively. Although these two compounds demonstrated a reduction in efflux rate compared with parent phenylalanine (70% and 74%, respectively), they were still significantly greater than negative control amino acids Gly and L-Arg (29% and 28%, respectively), suggesting that they are substrates of LAT1. Given the superior potency associated with hydrophobic groups at the meta position as in compounds **69** and **70**, it might not be surprising that a *tert*-butyl ester would present a higher affinity than a methyl ester. However, this line of reasoning is contradicted by the observation that the hydrophilic hydroxy group in **82** gave comparable activity. One possible explanation, as suggested by our models, is that the hydroxy group in 82 may be forming a hydrogen bond with residue Glu136 in the binding site to explain its unexpectedly good potency (Figure 3a). Moreover, though a phenolic hydroxy group in 71 and a benzyl alcohol in **73** were tolerated (IC_{50}s 130 and 83 μM, respectively), they did not demonstrate a boost in activity relative to phenylalanine as did **82**, which offers further evidence of a potential specific interaction for the latter.

Perhaps more surprisingly, compounds with aryl substituents which would be charged at pH 7.4 exhibited substrate activity. Specifically, benzyl amine **74** and carboxylic acid **83** both showed significant efflux rates (78% and 56%, respectively) indicating that they were LAT1 substrates. Although both benzyl amine **74** (IC_{50} 470 μM) and carboxylic acid **83** (IC_{50} 130 μM) were less potent than parent phenylalanine (IC_{50} 69 μM), they do maintain the ability to bind to the transporter. This is in sharp contrast to what we and others[1] have observed for nonsubstrate aliphatic amino acids containing basic or acidic side chains (i.e., Arg, Lys, Asp, and Glu), none of which were LAT1 substrates in our assays (Table 1). Although the synthesis of compound 83 has been reported, apparently it was not tested for LAT1 activity.[21] Thus, to the best of our knowledge, this is the first report of LAT1 substrates containing side chain substituents expected to be charged at pH 7.4. However, it should be noted that we cannot be certain whether they would be ionized within the ligand binding site. Despite tolerating a carboxylic acid directly attached to the meta-position (i.e., **83**), the SAR appears to be fairly narrow, in that analogue **84** containing a one-carbon spacer separating the carboxylic acid and aromatic ring, along with para-substituted **87**, were both nonsubstrates according to our *trans*-stimulation assay (24% and 20% relative to L-Phe efflux rate, respectively).

As previously noted, LAT1 has a preference for aromatic amino acids relative to aliphatic ones that is not directly correlated with lipophilicity[23,59] in spite of the fact that it also readily transports some bulkier, aliphatic amino acids such as leucine, valine, isoleucine, and methionine (Table 3). Similarly, we found that replacing the aromatic ring of phenylalanine

Author Manuscript Author Manuscript Author Manuscript Author Manuscript

with an unsaturated, cyclohexyl ring, as in **110** and **110-D** (Table 1), led to unexpectedly good activity in our *trans*stimulation assay (120% and 130%, respectively) while losing potency in our *cis*-inhibition assay (200 and 260 μM, respectively). From our models, we cannot say whether a π stacking interaction is taking place to enhance ligand affinity and/or if the planarity of the aromatic ring is optimal for binding to LAT1. However, aromaticity is clearly not required for substrate activity, provided that a hydrophobic side chain is present (e.g., L-Leu **46**, L-Val **49**, and cyclohexyl analogues **110** and **110-D**).

As para-substituted methyl ester **86** showed a dramatic loss in potency relative to the meta isomer **79** (IC_{50}s 260 vs 36 μM, respectively), we did not pursue further substitution at the para position. This difference in SAR for para vs meta substitution is consistent with our binding site models and those of others,[59,60] which predict less space is available near the para position. Synthetic attempts at placing a methyl ester at the ortho position were plagued by intramolecular cyclization via the α-amino group to give a lactam, thus *ortho* analogues were not pursued. Additionally, we previously showed that *ortho*-methyl substitution was inferior to *meta*-methyl substitution in terms of efflux rate (100% vs 140%, respectively).[56] Similarly, the d isomer of methyl ester **79** demonstrated a ~5-fold loss in activity and was potentially not a substrate due to its relatively low efflux rate (41%). Given the fact that both enantiomers of parent phenylalanine, **50** and **50-D**, have comparable efflux rates and IC_{50} values, the results for **79-D** suggest that its methyl ester is being forced to occupy a less favorable space in the binding site compared with **79**. However, our models do not provide an explanation for this difference in potency.

As indicated by modeling, there are two putative pockets near the aromatic ring of phenylalanine (i.e., PA and PB, Figure 1c) that might be filled to increase binding affinity. Our dockings suggested that one pocket was being filled by the various meta substituents of Table 1, while the second pocket, close to the other meta position, was left empty. Thus, we hypothesized that targeting both pockets simultaneously could increase substrate activity. To test this, we synthesized methyl-substituted analogues **63** and **64**. Regrettably, both compounds lost activity relative to their parent compounds **79** and 83. It is possible that our model does not account for subtle shifts in the residues in this region of the binding site which may disfavor substitution at both meta positions.

As most LAT1 substrates contain hydrophobic side chains, it has been intriguing to us that the relatively polar imidazole-containing L-histidine 53 is also a substrate and demonstrates high affinity.[50,61] Indeed, L-histidine appears to be an outlier in this regard, as it is considerably more hydrophilic compared with typical substrates (e.g., cLogP/tPSA: histidine = –3.7/88, phenylalanine = –1.6/63). We decided to explore the SAR around L-histidine **53** by preparing benzyl histidine **59** to test whether adding a lipophilic substituent could improve ligand potency (Table 1). Moreover, our models predicted that this Nim-benzyl group should be able to satisfactorily fill PA (Figure 3b). Although **59** along with smaller methyl-substituted **58** were both substrates based on our *trans*-stimulation assay (Table 1), they had diminished efflux rates and IC_{50} values relative to parent 53. Thus, contrary to what we expected, *Nim*-substitution on L-histidine **53** is detrimental for interaction with the binding site, though it does appear to be tolerated.

Author Manuscript Author Manuscript Author Manuscript Author Manuscript

Given the activity of L-histidine and these new histidine derivatives (i.e., **58** and **59**), we were curious as to whether pyridyl isomers **60**–**62** (Table 1) would also be substrates. To our satisfaction, **60**–**62** all demonstrated significant efflux rates in our *trans*-stimulation assay (89–140% relative to the efflux rate of L-Phe) and comparable IC_{50} values to L-phenylalanine (Table 1). Consistent with the SAR for substituted phenylalanine analogues, having the nitrogen in the meta position gave the top potency (61, IC_{50} = 69 μM) of the three isomers. To our knowledge, this is the first time these pyridyl analogues of L-phenylalanine have been tested against LAT1. In contrast to benzyl amine 74, none of these heterocyclic amino acids would be expected to carry a full positive charge at pH 7.4. This SAR is consistent with what we observed for polar-substituted phenylalanine analogues of Table 1, in that it corroborates the argument that LAT1 readily accommodates both polar and nonpolar aromatic rings.

Amino Acids D vs L.

As indicated above, some D-amino acids (i.e., Leu, Phe, and Met) have been shown to have substrate activity comparable to their L counterparts while others do not.[61] We speculated that the side chains of the more potent D enantiomers were comfortable binding in a narrow, hydrophobic pocket "C" (Figure 1c: PC), predicted by our models to be close to the α carbon. In contrast, this putative PC might not be able to accommodate the side chains of the less potent D-amino acids as readily as for Leu, Phe, and Met. To summarize, we imagined that upon binding L-amino acids, the region near pockets "A + B" (PA + PB) would typically be filled with an aromatic ring (Phe, Trp, His, Tyr) or bulky/hydrophobic alkyl group (Met, Leu, Ile, Val), while PC would be empty. On the other hand, we thought that D-amino acids might be filling PC with their side chains, leaving region PA + PB empty. Keeping this idea in mind, we hypothesized that substitution at the α position of phenylalanine with the side chains of Phe, Leu, and Met (compounds of Table 2) might allow both PA + PB and PC to be filled simultaneously, leading to improved potency.

Disappointingly, only three of the α-quaternary phenylalanine derivatives tested (Table 2) demonstrated substrate activity. Although both enantiomers of α-methyl phenylalanine **92** and **92-D** were substrates, they lost activity relative to parent phenylalanine. Furthermore, methionine's sulfide side chain (**98**) was tolerated at the α position; however, this compound also showed inferior activity relative to parent phenylalanine. Its enantiomer, **98-D**, lost all activity. On the basis of this SAR, it is impossible to say whether putative PC is being accessed by these α-quaternary analogues or whether our hypothesis that the side chains of D-amino acids are filling PC upon binding to LAT1 is incorrect, but we can say that substitution at the α position appears to be limited to relatively small groups, as both the benzyl and (lH-imidazol-4-yl)methyl analogues **93** and **107**, respectively, were inactive. Given the lack of activity for **107**, we decided not to prepare its d enantiomer, particularly because **107** involved a cumbersome, multistep synthesis (see Supporting Information). On the basis of our refined models and the SAR of Table 2, we now think that the geometry for α-substituted phenylalanine derivatives simply does not allow for optimal interaction with LAT1.

Author Manuscript Author Manuscript Author Manuscript Author Manuscript

Although it is known that LAT1 is nonstereoselective for transporting Phe, Met, and Leu,[61] it was unclear from the *cis*- inhibition assay results described by Yanagida[61] as to whether the D isomers of the other endogenous LAT1 substrates were simply weak binding substrates or not transported at all. As we are highly interested in better understanding LAT1 SAR, we decided to test both enantiomers of several naturally occurring amino acid substrates in our cell assays (Table 3). To our surprise, all of the D-amino acids tested, with the possible exception of D-Val (**49-D**), appear to be LAT1 substrates based on our *trans*-stimulation assay. As anticipated, both enantiomers of Phe and Met were substrates, with the D isomers of Met and Phe, **48-D** and **50-D**, respectively, having comparable IC_{50} values with their respective l enantiomers. This result is quite different from the previously reported K_m values for L-Phe and D-Phe, 14.2 and 121 μM, respectively.[61] Those experiments were performed using *Xenopus laevis* oocytes, which may explain this discrepancy. For amino acids Leu, Tyr, and Trp (**46**, **51**, and **52**, respectively), LAT1 showed a 2–3-fold greater selectivity for the L isomers in our *cis*-inhibition assay. Much greater stereoselectivity (>20-fold) was observed for Ile, Val, and His (**47**, **49**, and **53**, respectively). Given the relatively low efflux rate for D-Val (41%), we are not confident that it is a substrate. However, it clearly has poor affinity for the transporter relative to the other D-amino acids tested. From this SAR, one might deduce that the β-methyl groups of D-Val and D-Ile are poorly tolerated in the binding site. Likewise, the polar side chain of L-His is readily accommodated in LAT1, but with D-His, our data suggest it may be forced into an unfavorable position within the binding site.

On the basis of the data of Table 3, it is apparent that amino acid enantiomers (D vs L) have a different SAR regarding *cis*- inhibition even though they are not that different in their ability to cause a *trans*-stimulation effect. In agreement with the comparable V_{max} values previously reported for each pair of enantiomers of Leu and Phe,[61] we conclude from our assays that LAT1 is not stereoselective with regards to the rate of transporting amino acids, although the manner in which the D and L isomers bind to LAT1 appears to be quite different given their relative IC_{50}s.

Taken together, our SAR studies (Tables 1–3) indicate that the LAT1 binding site is surprisingly promiscuous. For example, we have shown that there is little correlation between meta-substituent polarity and ligand potency (Figure 2). However, we have also uncovered surprising variations in SAR such as loss in activity by adding a one carbon spacer going from **83** to **84** as well as dramatic differences in potency for some stereoisomer pairs but not others (e.g., histidine **53** vs phenylalanine **50**). Although our models have helped us to generate hypotheses for ligand design, and in a several cases offered a rationale for activity (e.g., differences between meta and para substitution and potential hydrogen bonding for polar substituents such as in **82**), they are currently unable to explain some of the divergent SAR that we have observed such as the differential activities of amino acid enantiomers. We are continuing to refine and improve our models as new LAT1 SAR becomes available.

Author Manuscript Author Manuscript Author Manuscript Author Manuscript

Chemistry.

Aryl-substituted phenylalanine analogues of Table 1 were prepared according to Scheme 1, using similar methodology as we previously employed.[56] Conversion of protected iodoalanine 5[85] to organozinc 6 using conditions which have been shown to maintain the chirality of the starting amino acid moiety as developed by Jackson[86,87] and later modified by Huo[88] was conducted in DMF, using catalytic I_2 to activate zinc prior to sonication and/or vigorous stirring with 5. We found that using THF as solvent gave considerable acrylate byproduct (~50%) due to elimination, presumably prior to forming 6. Nonetheless, acrylate remained a commonly observed byproduct (10–30% in ^{1}H NMR of the crude reaction mixture) using DMF. We confirmed the results of Jackson[89] that there was no loss in stereochemistry during formation of organozinc **6** and subsequent Negishi coupling in forming compounds 8 by preparing BOC/*tert*-butyl protected L-phenylalanine (i.e., R = Ph) using the current methodology (see Supporting Information). The resulting optical rotation of this compound matched what was previously reported in the literature for enantiomerically pure material prepared by a different route.[90]

Although aryl iodides have been more commonly reported as coupling partners than aryl bromides in Negishi reactions with analogues of **6**,[86,87,89,91–94] we preferred to prepare the desired phenylalanine analogues using the latter due to commercial availability. To determine the best catalyst system for formation of **8**, we compared ^{1}H NMR spectra of crude Negishi product mixtures after aqueous workup for various catalyst combinations using bromobenzene as a model coupling partner. On the basis of results by Paju,[85] we tested $Pd_2(dba)_3$/QPhos alongside other commonly used catalyst combinations, including $PdCl_2$(dppf) and $Pd(Ph_3P)_4$. We found that the latter two were vastly inferior, giving negligible amounts of desired 8. Combination of $Pd_2(dba)_3$ with ligands previously used in Negishi couplings of other substrates, SPhos[95] and CPhos,[96] gave significantly more desired **8** (20–30% of crude by ^{1}H NMR) but were inferior to QPhos[97] and P(*o*-tolyl)$_3$, which both gave ~50% of **8** present in the crude reaction mixture. Byproducts included acrylate from elimination of **5**, along with BOC-protected alanine *tert*-butyl ester, likely from protonation of uncoupled **6**, and 1–2 other unidentified compounds. As the latter two catalysts gave comparable results and due to the significantly lower cost of P(*o*-tolyl)$_3$, we proceeded to perform all Negishi reactions with this catalyst. Isolated yields (17–51%) for formation of each coupling product **8a–8o** are given in Table S3 (Supporting Information).

The primary reason for choosing the protecting groups depicted in Scheme 1 (i.e., *tert*-butyl ester and BOC) was that they could be conveniently and efficiently removed in a single step using TFA plus anisole as a carbocation scavenger.[98] In some cases, poor yields of the desired phenylalanine analogues were obtained (<20%), not necessarily because of the deprotection step but rather due to carry over of byproducts from the Negishi coupling reaction. All final products were obtained in high purity (>95% LC-MS) after preparative HPLC purification, which easily separated amino acids from anisole and other byproducts that were not removed after the Negishi coupling step. Saponification of aryl methyl esters in **63**, **79**, **80**, and **86** readily provided the corresponding carboxylic acid-substituted analogues **64**, **83**, **84**, and **87** in good yield (57–82%) after preparative HPLC purification.

Author Manuscript Author Manuscript Author Manuscript Author Manuscript

Alpha-substituted amino acids of Table 2 were prepared using "self-regeneration of chirality" methodology developed by Seebach, [99,100] which has been shown to give high diastereoselectivity (>97% de) for alkylation of enolates derived from either imidazolidinones or oxazolidinones (i.e., step b, Scheme 2).[101] At the outset, we selected the oxazolidinone system because of the ease of deprotection under relatively mild conditions.[102] Conversion of Cbz-L-phenylalanine to oxazolidinone **90** was performed by using a method developed by Karady[103] and later modified by Cheng.[104] Crystallization of 90 gave material that was a single diastereomer by ^{1}H NMR, with cis configuration as previously assigned.[104] Unfortunately, alkylation of **90** was problematic. We obtained <5% of the desired **91** when using isobutyl iodide as an electrophile. Presumably, the enolate of **90** decomposed more quickly than the alkylation event, as there was no evidence of **90** in the crude after allowing the reaction to slowly warm from –78 °C to rt over several hours, followed by aqueous workup. As ester enolates are known to be unstable giving rise to reactive ketene intermediates,[105] this should not have been too surprising. Fortunately, we found that by increasing the reactivity of the electrophile by using isobutyl triflate, we were able to obtain a good yield (72%) of **91** that appeared to be a single diastereomer by ^{1}H NMR. Deprotection using $KOSiMe_3$ as developed by Coe[102] simultaneously removed the oxazolidinone and Cbz protecting groups in reasonable yield (55% of **94** after preparative HPLC purification). The synthesis of Scheme 2 was repeated starting with the D isomer of phenylalanine to give the opposite enantiomer **94-D**. To determine enantiopurity of the final products, their amino groups were acylated with acetic anhydride and chiral HPLC analysis was performed on both enantiomers (Supporting Information). Although compound 94 was obtained in 98% ee, its isomer **94-D** was obtained in only 86% ee using the same synthesis. It is unclear to us how this reduction in stereochemical integrity took place given the fact that oxazolidinone precursor **90-D** appeared to be a single diastereomer by ^{1}H NMR. Nonetheless, our conclusions concerning SAR were not affected by this discrepancy. To our knowledge, this is the first synthesis, racemic or enantioselective, of α-isobutyl phenylalanine, probably due to the challenges associated with forming such a sterically congested molecule. Also, we found that alkylation of **90** with isopropyl triflate could be performed, albeit with significantly poorer yield (17%). However, purification issues at the final step and the lack of activity for **94** and **94-D** (Table 2) deterred us from completing the synthesis of the planned α-isopropyl phenylalanine analogues.

Although the chemistry of Scheme 2 provided the desired isobutyl-substituted phenylalanine analogues **94** and **94-D**, we were unable to apply this methodology to more functionalized derivatives (e.g., compounds **98** and **107**). The analogous triflates, 2-(methylthio)ethyl triflate and protected versions of (1H-imidazol-4-yl)methyl triflate, are not known in the literature, likely due to the presence of internal nucleophiles which would not be compatible with the highly reactive alkyl triflate group. In fact, when we attempted to prepare trityl-protected (1H-imidazol-4-yl)methyl triflate from the corresponding alcohol and triflic anhydride using pyridine as base, we obtained a highly complex mixture. Thus, we explored taking an alternate approach for introduction of the α-substituent by preparing the phenyl-substituted oxazolidinones (as present in **90**) of both methionine and histidine, with the idea of alkylation using either benzyl iodide or benzyl triflate to prepare the desired α-quaternary amino acids **98** and **107**, respectively. However, this approach was also problematic. We

Author Manuscript Author Manuscript Author Manuscript Author Manuscript

were unable to separate diastereomers of the methionine version of 90, and we failed to obtain the histidine-derived analogue of 90 using the given reaction conditions, probably due to incompatibility of Cbz-trityl-protected histidine with BF_3—Et_2O. Rather than spend more time exploring various conditions solely for the sake of using the same methodology as for **94**, we opted to prepare compounds **98** and **107** according to their previously described stereoselective syntheses from the literature. These published routes involved diastereoselective alkylation with benzyl iodide of a methionine-derived tert-butyl-substituted oxazolidinone[82] and a histidine-derived tert-butyl-substituted imidazolidinone[83,84] for **98** and **107**, respectively (see Supporting Information for full experimental details). The enantiomeric purities of compounds **98** and **98-D** (78% ee and 80% ee, respectively, as determined by chiral HPLC analysis of the acetylated amino acids) were consistent with what was observed in the previously reported synthesis.[82] Apparently alkylation of the oxazolidinone intermediate in this case is not entirely stereoselective (see Supporting Information). The enantio-purity of inactive (1*H*-imidazol-4-yl)methyl analogue **107** was not determined.

CONCLUSION

We have developed a new structural model of human LAT1 to visualize the interactions between substrates and inhibitors with the binding site. Using a combined approach of ligand-and structure-guided design, we have identified several novel LAT1 substrates and inhibitors, thereby revealing specificity determinants that will be useful for future drug design. From our SAR studies, it is apparent that LAT1 is considerably more tolerant of polar and even ionizable functional groups in the ligand's side chain than what had previously been described in the literature. Further, the transporter is capable of transporting both L and D enantiomers, albeit with varying IC_{50}s depending on the amino acid. These findings could influence the design of new drug delivery agents or inhibitors targeting LAT1. On the basis of our refined SAR models, we are currently in the process of designing amino acid-containing prodrugs that utilize this SAR to improve their uptake into cancer cells and to cross the BBB.

EXPERIMENTAL SECTION

Chemistry.

All final, tested compounds were ≥95% purity by LC-MS analysis. Most of the naturally occurring **l-** and D-amino acids were purchased from commercial suppliers and converted to their HCl salts to improve water solubility (Gly, Leu, Ile, Met, Val, Phe, Tyr, Trp, His; whereas, Arg, Lys, Asp, and Glu were tested in their zwitterionic form) by suspension in 1,4-dioxane and addition of 1.1 equiv (2.1 equiv for His) of 4 N HCl in 1,4-dioxane, followed by concentration in vacuo and drying overnight under high vacuum prior to testing in cell assays. The following non-natural amino acids were purchased from these vendors: Santa Cruz (58), Molport (**59**), Alfa Aesar (pyridyl isomers **60**, **61**, **62**, and **65**), Combi-Blocks (71), Chem-Impex (**85**, **92**, **92-D**, and **110**), Enamine (**93**, purchased and tested as the hydrobromide salt), and Oakwood (**110-D**). All purchased, tested compounds were analyzed by LC-MS to confirm identity and purity (>95%), and for chiral compounds, enantiopurity

Author Manuscript Author Manuscript Author Manuscript Author Manuscript

was verified by optical rotation and comparison with literature values (Supporting Information). The syntheses of compounds 68, 69, and 70 have previously been published.[56]

Preparative HPLC performed on a Gilson PLC 2020. Column: Synergi 4 μ Fusion-RP by Phenomenex, 150 mm × 21.2 mm. LC-MS analysis was performed using an Agilent G6125 single quad ESI source and a 1260 Infinity HPLC system (G7112B binary pump and G7114A dual $\boldsymbol{\lambda}$ absorbance detector). Column: Synergi 4 μ Fusion-RP by Phenomenex, 150 mm × 4.6 mm. ^{1}H and ^{13}C NMR were recorded on an Avance III HD Bruker instrument operating at 400 and 100 MHz, respectively. HRMS analysis (TOF ES+) was performed on a Micromass Q-Tof Ultima mass spectrometer. Optical rotations were measured on a Rudolph Research Autopol III polarimeter (using sodium D line, 589 nm) and $[\boldsymbol{\alpha}]_{\mathrm{D}}$ given in units of (degrees-mL)/(dm-g), and concentration ($\boldsymbol{c}$) is reported in units of g/100 mL. Further details on specific experimental techniques, methods of analysis, and full procedures and analytical data for compounds are provided in Supporting Information.

Cell Culture and Characterization.

TREx HEK-hLAT 1 (XenoPort, Inc., Santa Clara, CA) is an inducible cell line which is under control of a tetracycline inducible promoter. Besides LAT1, this cell line also has a second tetracycline inducible plasmid encoding 4F2hc (SLC3A2). LAT1 and 4F2hc will form a heterodimer leading to transport of its substrates.[70,106] Genetic disruption of either LAT1 or 4F2hc abolishes uptake activity,[28] which demonstrates that both components are important for LAT1 transport function. To induce maximal expression of LAT1 and 4F2hc, doxycycline (Dox) and a histone deacetylase (HDAC) inhibitor, sodium butyrate, were added simultaneously in the media. As previously described,[17] TREx HEK 293 cells (purchased from Invitrogen) were cotransfected with a plasmid encoding hLAT1 under control of a tetracycline inducible promoter and a second tetracycline inducible plasmid encoding h4F2hc, using Fugene transfection reagent following manufacturer's instructions (Roche Biosciences). These cells were grown and maintained in Dulbecco's Modified Eagle Medium (DMEM) H-21 media supplemented with 10% fetal bovine serum, 100 units/mL penicillin, 100 units/mL streptomycin, 1 μg/mL Fungizone, 2 mM L-glutamine, and 3 μg/mL blasticidin. Cells were grown at 37 °C in a humidified incubator with 5% CO_2. After thawing a fresh vial, cells were used for a maximum of 15 passages in this study. The presence of functional LAT1 in HEK hLAT1 cells has been previously established,[74] as it was shown that the uptake of the known substrates L-phenylalanine, L-DOPA, and gabapentin corresponded with their relative LAT1 affinities as described for other cell lines.[14,16,61,107] Uptake of [^{3}H]-gabapentin into induced HEK-hLAT1 cells (Supporting Information, Figure S2) was verified prior to each cell assay.

cis-Inhibition Assay and IC50 Determinations.

HEK-hLAT1 cells were grown on poly-D-lysine coated 24-well plates in DMEM medium described above to at least 90% confluence at 48 h postseeding. Then 24 h before the experiment, cells were treated with **1** $\boldsymbol{\mu}$g/mL doxycycline and 2 mM sodium butyrate to induce expression of hLAT1. On the day of the experiment, cells were washed and preincubated in prewarmed, sodium-free choline buffer (140 mM choline chloride, 2 mM potassium chloride, 1 mM magnesium chloride, 1 mM calcium chloride, 1 M Tris) for 10

Author Manuscript Author Manuscript Author Manuscript Author Manuscript

min. The buffer was removed and replaced with uptake buffer (sodium-free choline buffer containing 6 nM of [^{3}H]-gabapentin) and each inhibitor at 200 μM. For IC_{50} determinations, varying concentrations of each inhibitor were added from 0.1 to 500 μM. Uptake was performed at 37 °C for 3 min and then terminated by washing the cells twice with ice-cold choline buffer. Cells were lysed by the addition of 800 μL of lysis buffer (0.1 N NaOH, 0.1% SDS) and allowed to sit at room temperature for 3 h. Intracellular radioactivity was determined by scintillation counting on a LS6500 scintillation counter (Beckman Coulter). IC_{50} and standard deviation of each compound were analyzed using Graphpad Prism version 5.0. %[^{3}H]-gabapentin uptake at each concentration was normalized relative to % inhibition by BCH[80,81] at 2 mM, which was set to 100% inhibition.

trans-Stimulation Assay.

HEK-hLAT1 cells were grown on poly-D-lysine coated 24-well plates in DMEM medium described above to at least 90% confluence at 48 h postseeding. Then 24 h before the experiment, cells were treated with 1 μg/mL doxycycline and 2 mM sodium butyrate to induce expression of hLATl. On the day of the experiment, cells were washed with prewarmed, sodium-free choline buffer (140 mM choline chloride, 2 mM potassium chloride, 1 mM magnesium chloride, 1 mM calcium chloride, 1 M Tris), then incubated in the same preincubation solution containing 6 nM of [^{3}H]-gabapentin.[108] After 30 min, the preincubation solution was quickly removed and cells were washed twice with sodium-free choline buffer to remove extracellular radioactivity. Fresh sodium-free choline buffer containing each of the tested compounds at 200 μM were added to the cells, and an aliquot of the buffer was obtained at 3 min after addition of the test compound. NOTE: There is precedent in other published assays where high ratios (i.e., 100- to >1000-fold) of test compound to radiolabel have been used to ensure saturation of the transporter by the test compound.[26,58,75,78,109,110] Furthermore, as the exchange ratio for LAT1 has been established as a 1:1 stoichiometry,[79] the amount of effluxed radiolabel should match the amount of test substrate taken into the cell by LAT1, regardless of the extracellular concentration of the test compound. The extracellular radioactivity was determined by scintillation counting on a LS6500 scintillation counter (Beckman Coulter). Efflux of [^{3}H]-gabapentin was calculated at 3 min after adding test compound. Percent efflux was normalized relative to L-Phe (compound 50), which had an efflux rate of 2.7 ± 0.3 fmol/min, from an average of seven experiments.

Homology Modeling and Ligand Docking.

We used homology models of LAT1 in two distinct conformations: (i) a previously published model of the outward-occluded conformation of AdiC from *Echerichia coli* (PDB 3L1L) and (ii) a new model of LAT1 that we generated based on a recently determined structure of the *E.coli* AdiC in the outward-open conformation (PDB 5J4N[71]). This outward-open model was built using MODELLER with the same target-template alignment. The Z-DOPE scores of the models were −0.318 and −0.531, respectively, suggesting that 60–70% of their C_α are within 3.5 Å of their native distance and are thus expected to be sufficiently accurate for further analysis (both the open and occluded models can be downloaded online: http://www.schlessingerlab.org/data/). Additional details on homology modeling and ligand docking can be found in the Supporting Information.

Author Manuscript Author Manuscript Author Manuscript Author Manuscript

Pan-Assay Interference Compounds (PAINS) Screen.

The ZINC15 PAINS-Aggregator online web server (http://zinc15.docking.org/patterns/home/) was used to check compounds of Tables 1–3 for the likelihood of interference in our cell assays.[111] Only the enantiomers of the amino acid histidine (**53** and **53-D**) and ***α***-methylphenylalanine (**92** and **92-D**) were flagged as potential aggregators. Given the activity of these compounds in two separate assays (***cis***-inhibition and *trans*-stimulation), which is consistent with the SAR trends for the other amino acids tested, it is improbable that their activity is due to assay interference. Moreover, if they were forming aggregates, it is unlikely that they would be able to exchange with [^{3}H]-gabapentin in our *trans*-stimulation assay. Additionally, both L-histidine and ***α***-methylphenylalanine are known LAT1 substrates, and our IC_{50} values are consistent with previously reported results.[4,61]

Supplementary Material

Refer to Web version on PubMed Central for supplementary material.

ACKNOWLEDGMENTS

K.F., S.S., L.S., E.A., A.F., L.H., and A.A. thank the University of Nebraska at Kearney (UNK) University Research Fellows (URF) Program for financial support. E.A., S.S., and A.F. also thank the UNK Summer Student Research Program (SSRP). This work was supported by the National Institutes of Health grant R15 NS099981 (to A.A.T), the UNK Research Services Council (RSC), and the Nebraska EPSCoR Undergraduate Research Experiences (URE) Program. We appreciate Open-Eye Scientific Software Inc. for granting us access to its high-performance molecular modeling applications through its academic license program. This work was supported in part by the National Institutes of Health's National Institute of General Medical Sciences grant U01 GM61390 (to H.C.C., A.A.Z., and K.M.G.) and R01 GM108911 (to A.S. and C.C.). Finally, financial support from the University of Bern and the National Centre of Competence in Research (NCCR) TransCure to D.F. is gratefully acknowledged. A.A.T. wants to thank UNK freshmen chemistry apprentices Alyssa Wells, Joseph Griffith, Hannah Wolfe, Cesar Alvarado, Alex Duncan, Hannah Way, and Kasey Merklin for their assistance in measuring optical rotation values and with NMR and LC-MS analysis.

ABBREVIATIONS USED

LAT1	L-type amino acid transporter 1
APC	amino acid-polyamine-organocation
TM	transmembrane helix
BCH	2-aminobicyclo[2.2.1]heptane-2-carboxylic acid
dba	dibenzyli-deneacetone
dppf	1,1′-bis(diphenylphosphino)ferrocene
QPhos	pentaphenyl(ditert-butylphosphino)ferrocene
CPhos	2-(2-dicyclohexylphosphanylphenyl)-*N*1,*N*1,*N*3,*N*3-tetrameth-yl-benzene-1,3-diamine
SPhos	2-dicyclohexylphosphino-2′,6′-dimethoxybiphenyl
DMEM	Dulbecco's Modified Eagle Medium

Author Manuscript Author Manuscript Author Manuscript Author Manuscript

DOPE	discrete optimized protein energy
FRED	fast exhaustive docking

REFERENCES

(1). Kanai Y; Segawa H; Miyamoto K; Uchino H; Takeda E; Endou H Expression cloning and characterization of a transporter for large neutral amino acids activated by the heavy chain of 4F2 antigen (CD98). J. Biol. Chem. 1998, 273, 23629–23632. [PubMed: 9726963]

(2). Boado RJ; Li JY; Nagaya M; Zhang C; Pardridge WM Selective expression of the large neutral amino acid transporter at the blood-brain barrier. Proc. Natl. Acad. Sci. U. S. A. 1999, 96, 12079–12084. [PubMed: 10518579]

(3). Kido Y; Tamai I; Uchino H; Suzuki F; Sai Y; Tsuji A Molecular and functional identification of large neutral amino acid transporters LAT1 and LAT2 and their pharmacological relevance at the blood-brain barrier. J. Pharm. Pharmacol. 2001, 53, 497–503. [PubMed: 11341366]

(4). Uchino H; Kanai Y; Kim DK; Wempe MF; Chairoungdua A; Morimoto E; Anders MW; Endou H Transport of amino acid-related compounds mediated by L-type amino acid transporter 1 (LAT1): Insights into the mechanisms of substrate recognition. MoZ. Pharmacol. 2002, 61, 729–737.

(5). del Amo EM; Urtti A; Yliperttula M Pharmacokinetic role of L-type amino acid transporters LAT1 and LAT2. Eur. J. Pharm. Sci. 2008, 35, 161–174.

(6). Sanchez-Covarrubias L; Slosky LM; Thompson BJ; Davis TP; Ronaldson PT Transporters at CNS barrier sites: Obstacles or opportunities for drug delivery? Curr. Pharm. Des. 2014, 20, 1422–1449. [PubMed: 23789948]

(7). Yanagisawa N; Satoh T; Hana K; Ichinoe M; Nakada N; Endou H; Okayasu I; Murakumo Y L-amino acid transporter 1 may be a prognostic marker for local progression of prostatic cancer under expectant management. Cancer Biomarkers 2015, 15, 365–374. [PubMed: 25835180]

(8). Kobayashi H; Ishii Y; Takayama T Expression of L-type amino acid transporter 1 (LAT1) in esophageal carcinoma. J. Surg. Oncol. 2005, 90, 233–238. [PubMed: 15906366]

(9). Ebara T; Kaira K; Saito J; Shioya M; Asao T; Takahashi T; Sakurai H; Kanai Y; Kuwano H; Nakano T L-type amino-acid transporter 1 expression predicts the response to preoperative hyperthermo-chemoradiotherapy for advanced rectal cancer. Anti-cancer Res. 2010, 30, 4223–4227.

(10). Ichinoe M; Mikami T; Yoshida T; Igawa I; Tsuruta T; Nakada N; Anzai N; Suzuki Y; Endou H; Okayasu I High expression of L-type amino-acid transporter 1 (LAT1) in gastric carcinomas: Comparison with non-cancerous lesions. Pathol. int. 2011, 61, 281–289. [PubMed: 21501294]

(11). Takeuchi K; Ogata S; Nakanishi K; Ozeki Y; Hiroi S; Tominaga S; Aida S; Matsuo H; Sakata T; Kawai T LAT1 expression in non-small-cell lung carcinomas: Analyses by semi-quantitative reverse transcription-PCR (237 cases) and immunohis-tochemistry (295 cases). Lung Cancer 2010, 68, 58–65. [PubMed: 19559497]

(12). Although histidine is frequently categorized as a basic amino acid, its side chain (pK = 6.0) would be mostly neutral at pH 7.4.

(13). Kageyama T; Nakamura M; Matsuo A; Yamasaki Y; Takakura Y; Hashida M; Kanai Y; Naito M; Tsuruo T; Minato N; Shimohama S The 4F2hc/LAT1 complex transports L-DOPA across the blood-brain barrier. Brain Res. 2000, 879, 115–121. [PubMed: 11011012]

(14). Soares-da-Silva P; Serrao MP High- and low-affinity transport of L-leucine and L-DOPA by the hetero amino acid exchangers LAT1 and LAT2 in LLC-PK1 renal cells. Am. J. Physiol. Renal Physiol 2004, 287, F252–261. [PubMed: 15271688]

(15). Wang Y; Welty DF The simultaneous estimation of the influx and efflux blood-brain barrier permeabilities of gabapentin using a microdialysis-pharmacokinetic approach. Pharm. Res. 1996, 13, 398–403. [PubMed: 8692732]

(16). Dickens D; Webb SD; Antonyuk S; Giannoudis A; Owen A; Radisch S; Hasnain SS; Pirmohamed M Transport of gabapentin by LAT1 (SLC7A5). Biochem. Pharmacol. 2013, 85, 1672–1683. [PubMed: 23567998]

Author Manuscript Author Manuscript Author Manuscript Author Manuscript

(17). Roberts LM; Black DS; Raman C; Woodford K; Zhou M; Haggerty JE; Yan AT; Cwirla SE; Grindstaff KK Subcellular localization of transporters along the rat blood-brain barrier and blood-cerebral-spinal fluid barrier by in vivo biotinylation. Neuroscience 2008, 155, 423–438. [PubMed: 18619525]

(18). Gynther M; Laine K; Ropponen J; Leppanen J; Mannila A; Nevalainen T; Savolainen J; Jarvinen T; Rautio J Large neutral amino acid transporter enables brain drug delivery via prodrugs. J. Med. Chem. 2008, 51, 932–936. [PubMed: 18217702]

(19). Killian DM; Hermeling S; Chikhale PJ Targeting the cerebrovascular large neutral amino acid transporter (LAT1) isoform using a novel disulfide-based brain drug delivery system. Drug Delivery 2007, 14, 25–31. [PubMed: 17107928]

(20). Walker I; Nicholls D; Irwin WJ; Freeman S Drug delivery via active transport at the blood-brain barrier: Affinity of a prodrug of phosphonoformate for the large amino acid transporter. int. J. Pharm. 1994, 104, 157–167.

(21). Peura L; Malmioja K; Huttunen K; Leppanen J; Hamalainen M; Forsberg MM; Rautio J; Laine K Design, synthesis and brain uptake of LAT1-targeted amino acid prodrugs of dopamine. Pharm. Res. 2013, 30, 2523–2537. [PubMed: 24137801]

(22). Rautio J; Gynther M; Laine K LAT1-mediated prodrug uptake: A way to breach the blood-brain barrier? Ther. Delivery 2013, 4, 281–284.

(23). Puris E; Gynther M; Huttunen J; Petsalo A; Huttunen KM L-type amino acid transporter 1 utilizing prodrugs: How to achieve effective brain delivery and low systemic exposure of drugs. J. Controlled Release 2017, 261, 93–104.

(24). Huttunen KM; Huttunen J; Aufderhaar I; Gynther M; Denny WA; Spicer JA L-type amino acid transporter 1 (LAT1)-mediated targeted delivery of perforin inhibitors. int. J. Pharm. 2016, 498, 205–216. [PubMed: 26705152]

(25). Kongpracha P; Nagamori S; Wiriyasermkul P; Tanaka Y; Kaneda K; Okuda S; Ohgaki R; Kanai Y Structure-activity relationship of a novel series of inhibitors for cancer type transporter L-type amino acid transporter 1 (LAT1). J. Pharmacol. Sci. 2017, 133, 96–102. [PubMed: 28242177]

(26). Nagamori S; Wiriyasermkul P; Okuda S; Kojima N; Hari Y; Kiyonaka S; Mori Y; Tominaga H; Ohgaki R; Kanai Y Structure-activity relations of leucine derivatives reveal critical moieties for cellular uptake and activation of mTORCl-mediated signaling. Amino Acids 2016, 48, 1045–1058. [PubMed: 26724922]

(27). Jin SE; Jin HE; Hong SS Targeting L-type amino acid transporter 1 for anticancer therapy: Clinical impact from diagnostics to therapeutics. Expert Opin. Ther. Targets 2015, 19, 1319–1337. [PubMed: 25968633]

(28). Cormerais Y; Giuliano S; LeFloch R; Front B; Durivault J; Tambutte E; Massard PA; de la Ballina LR; Endou H; Wempe MF; Palacin M; Parks SK; Pouyssegur J Genetic disruption of the multifunctional CD98/LAT1complex demonstrates the key role of essential amino acid transport in the control of mTORC1 and tumor growth. Cancer Res. 2016, 76, 4481–4492. [PubMed: 27302165]

(29). Honjo H; Kaira K; Miyazaki T; Yokobori T; Kanai Y; Nagamori S; Oyama T; Asao T; Kuwano H Clinicopathological significance of LAT1 and ASCT2 in patients with surgically resected esophageal squamous cell carcinoma. J. Surg. Oncol. 2016, 113, 381–389. [PubMed: 26936531]

(30). Shimizu A; Kaira K; Kato M; Yasuda M; Takahashi A; Tominaga H; Oriuchi N; Nagamori S; Kanai Y; Oyama T; Asao T; Ishikawa O Prognostic significance of L-type amino acid transporter 1 (LAT1) expression in cutaneous melanoma. Melanoma Res. 2015, 25, 399–405. [PubMed: 26237765]

(31). Yazawa T; Shimizu K; Kaira K; Nagashima T; Ohtaki Y; Atsumi J; Obayashi K; Nagamori S; Kanai Y; Oyama T; Takeyoshi I Clinical significance of coexpression of L-type amino acid transporter 1 (LAT1) and ASC amino acid transporter 2 (ASCT2) in lung adenocarcinoma. Am. J. Transl Res. 2015, 7, 1126–1139. [PubMed: 26279756]

(32). Kaira K; Arakawa K; Shimizu K; Oriuchi N; Nagamori S; Kanai Y; Oyama T; Takeyoshi I Relationship between CD147 and expression of amino acid transporters (LAT1 and ASCT2) in patients with pancreatic cancer. Am. J. Transl. Res. 2015, 7, 356–363. [PubMed: 25901202]

Author Manuscript Author Manuscript Author Manuscript Author Manuscript

(33). Namikawa M; Kakizaki S; Kaira K; Tojima H; Yamazaki Y; Horiguchi N; Sato K; Oriuchi N; Tominaga H; Sunose Y; Nagamori S; Kanai Y; Oyama T; Takeyoshi I; Yamada M Expression of amino acid transporters (LAT1, ASCT2 and xCT) as clinical significance in hepatocellular carcinoma. Hepatol. Res. 2015, 45, 1014–1022. [PubMed: 25297701]

(34). Wang J; Chen X; Su L; Li P; Liu B; Zhu Z LAT-1 functions as a promotor in gastric cancer associated with clinicopathologic features. Biomed. Pharmacother. 2013, 67, 693–699. [PubMed: 23809372]

(35). Yun D-W; Lee SA; Park M-G; Kim J-S; Yu S-K; Park M-R; Kim S-G; Oh J-S; Kim CS; Kim H-J; Kim J-S; Chun HS; Kanai Y; Endou H; Wempe MF; Kim DK JPH203, an L-type amino acid transporter 1-selective compound, induces apoptosis of YD-38 human oral cancer cells. J. Pharmacol. Sci. 2014, 124, 208–217. [PubMed: 24492461]

(36). Imai H; Kaira K; Oriuchi N; Shimizu K; Tominaga H; Yanagitani N; Sunaga N; Ishizuka T; Nagamori S; Promchan K; Nakajima T; Yamamoto N; Mori M; Kanai Y Inhibition of L-type amino acid transporter 1 has antitumor activity in non-small cell lung cancer. Anticancer Res. 2010, 30, 4819–4828. [PubMed: 21187458]

(37). Oda K; Hosoda N; Endo H; Saito K; Tsujihara K; Yamamura M; Sakata T; Anzai N; Wempe MF; Kanai Y; Endou H L-type amino acid transporter 1 inhibitors inhibit tumor cell growth. Cancer Sci. 2010, 101, 173–179. [PubMed: 19900191]

(38). Kim CS; Moon IS; Park JH; Shin WC; Chun HS; Lee SY; Kook JK; Kim HJ; Park JC; Endou H; Kanai Y; Lee BK; Kim DK Inhibition of L-type amino acid transporter modulates the expression of cell cycle regulatory factors in KB oral cancer cells. Biol. Pharm. Bull. 2010, 33, 1117–1121. [PubMed: 20606299]

(39). Shennan DB; Thomson J Inhibition of system l (LAT1/CD98hc) reduces the growth of cultured human breast cancer cells. Oncol. Rep. 2008, 20, 885–889. [PubMed: 18813831]

(40). Huttunen KM; Gynther M; Huttunen J; Puris E; Spicer JA; Denny WA A selective and slowly reversible inhibitor of L-type amino acid transporter 1 (LAT1) potentiates anti-proliferative drug efficacy in cancer cells. J. Med. Chem. 2016, 59, 5740–5751. [PubMed: 27253989]

(41). Napolitano L; Scalise M; Koyioni M; Koutentis P; Catto M; Eberini I; Parravicini C; Palazzolo L; Pisani L; Galluccio M; Console L; Carotti A; Indiveri C Potent inhibitors of human LAT1 (SLC7A5) transporter based on dithiazole and dithiazine compounds for development of anticancer drugs. Biochem. Pharmacol. 2017, 143, 39–52. [PubMed: 28709952]

(42). Park K Insight into brain-targeted drug delivery via LAT1-utilizing prodrugs. J. Controlled Release 2017, 261, 368.

(43). Bhunia S; Vangala V; Bhattacharya D; Ravuri HG; Kuncha M; Chakravarty S; Sistla R; Chaudhuri A Large amino acid transporter 1 selective liposomes of L-DOPA functionalized amphiphile for combating glioblastoma. Mol. Pharmaceutics 2017, 14, 3834–3847.

(44). Ong ZY; Chen S; Nabavi E; Regoutz A; Payne DJ; Elson DS; Dexter DT; Dunlop IE; Porter AE Multibranched gold nanoparticles with intrinsic LAT-1 targeting capabilities for selective photothermal therapy of breast cancer. ACS Appl Mater. Interfaces 2017, 9, 39259–39270. [PubMed: 29058874]

(45). Li L; Di X; Zhang S; Kan Q; Liu H; Lu T; Wang Y; Fu Q; Sun J; He Z Large amino acid transporter 1 mediated glutamate modified docetaxel-loaded liposomes for glioma targeting. Colloids Surf., B 2016, 141, 260–267.

(46). Li L; Di X; Wu M; Sun Z; Zhong L; Wang Y; Fu Q; He Z; Kan Q; Sun J Targeting tumor highly-expressed LAT1 transporter with amino acid-modified nanoparticles: Toward a novel active targeting strategy in breast cancer therapy. Nanomedicine 2017, 13, 987–998. [PubMed: 27890657]

(47). Smith QR Carrier-mediated transport to enhance drug delivery to brain. Int. Congr. Ser. 2005, 1277, 63–74.

(48). Tashima T Intriguing possibilities and beneficial aspects of transporter-conscious drug design. Bioorg. Med. Chem. 2015, 23, 4119–4131. [PubMed: 26138194]

(49). Morris ME; Guan X The role of transporters in drug delivery and excretion In Drug Delivery: Principles and Applications, 2nd ed.; Wang B, Hu L, Siahaan TJ, Eds.; John Wiley & Sons, Inc.: Hoboken, NJ, 2016; pp 62–102.

Author Manuscript Author Manuscript Author Manuscript Author Manuscript

(50). Smith QR Transport of glutamate and other amino acids at the blood-brain barrier. J. Nutr. 2000, 130, 1016S–1022S. [PubMed: 10736373]

(51). Ylikangas H; Malmioja K; Peura L; Gynther M; Nwachukwu EO; Leppanen J; Laine K; Rautio J; Lahtela-Kakkonen M; Huttunen KM; Poso A Quantitative insight into the design of compounds recognized by the L-type amino acid transporter 1 (LAT1). ChemMedChem 2014, 9, 2699–2707. [PubMed: 25205473]

(52). Nasset ES; Heald FP; Calloway DH; Margen S; Schneeman P Amino acids in human blood plasma after single meals of meat, oil, sucrose and whiskey. J. Nutr. 1979, 109, 621–630. [PubMed: 571014]

(53). Alexander GM; Schwartzman RJ; Grothusen JR; Gordon SW Effect of plasma levels of large neutral amino acids and degree of Parkinsonism on the blood-to-brain transport of levodopa in naive and MPTP Parkinsonian monkeys. Neurology 1994, 44, 1491–1499. [PubMed: 8058155]

(54). Karobath M; Diaz JL; Huttunen MO The effect of L-DOPA on the concentrations of tryptophan, tyrosine and serotonin in rat brain. Eur. J. Pharmacol. 1971, 14, 393–396. [PubMed: 5157767]

(55). Cheng Z; Liu Q Uptake transport at the BBB-examples and SAR In Blood-Brain Barrier in Drug Discovery: Optimizing Brain Exposure of CNS Drugs and Minimizing Brain Side Effects for Peripheral Drugs, 1st ed.; Di L, Kerns EH, Eds.; John Wiley & Sons: Hoboken, NJ, 2015; pp 138–145.

(56). Augustyn E; Finke K; Zur AA; Hansen L; Heeren N; Chien H-C; Lin L; Giacomini KM; Colas C; Schlessinger A; Thomas AA LAT-1 activity of meta-substituted phenylalanine and tyrosine analogs. Bioorg. Med. Chem. Lett. 2016, 26, 2616–2621. [PubMed: 27106710]

(57). Zur AA; Chien H-C; Augustyn E; Flint A; Heeren N; Finke K; Hernandez C; Hansen L; Miller S; Lin L; Giacomini KM; Colas C; Schlessinger A; Thomas AA LAT1 activity of carboxylic acid bioisosteres: Evaluation of hydroxamic acids as substrates. Bioorg. Med. Chem. Lett. 2016, 26, 5000–5006. [PubMed: 27624080]

(58). Geier EG; Schlessinger A; Fan H; Gable JE; Irwin JJ; Sali A; Giacomini KM Structure-based ligand discovery for the large-neutral amino acid transporter 1, LAT-1. Proc. Nat/. Acad. Sci. U. S. A. 2013, 110, 5480–5485.

(59). Ylikangas H; Peura L; Malmioja K; Leppanen J; Laine K; Poso A; Lahtela-Kakkonen M; Rautio J Structure-activity relationship study of compounds binding to large amino acid transporter 1 (LAT1) based on pharmacophore modeling and in situ rat brain perfusion. Eur. J. Pharm. Sci. 2013, 48, 523–531. [PubMed: 23228412]

(60). Peura L; Malmioja K; Laine K; Leppanen J; Gynther M; Isotalo A; Rautio J Large amino acid transporter 1 (LAT1) prodrugs of valproic acid: New prodrug design ideas for central nervous system delivery. Mol. Pharmaceutics 2011, 8, 1857–1866.

(61). Yanagida O; Kanai Y; Chairoungdua A; Kim DK; Segawa H; Nii T; Cha SH; Matsuo H; Fukushima J; Fukasawa Y; Tani Y; Taketani Y; Uchino H; Kim JY; Inatomi J; Okayasu I; Miyamoto K; Takeda E; Goya T; Endou H Human L-type amino acid transporter 1 (LAT1): Characterization of function and expression in tumor cell lines. Biochim. Biophys. Acta, Biomembr. 2001, 1514, 291–302.

(62). Ohshima Y; Hanaoka H; Tominaga H; Kanai Y; Kaira K; Yamaguchi A; Nagamori S; Oriuchi N; Tsushima Y; Endo K; Ishioka NS Biological evaluation of 3-[(18)F]fluoro-alpha-methyl-D-tyrosine (D-[(18)F]FAMT) as a novel amino acid tracer for positron emission tomography. Ann. Nucl. Med. 2013, 27, 314–324. [PubMed: 23337966]

(63). Uchino H; Yoshikatsu K; Kyung Kim D; Wempe MF; Chairoungdua A; Morimoto E; Anders MW; Endou H Transport of amino acid-related compounds mediated by L-type amino acid transporter 1 (LAT1): Insights into the mechanisms of substrate recognition. Mol. Pharmacol. 2002, 61, 729–737. [PubMed: 11901210]

(64). Mastroberardino L; Spindler B; Pfeiffer R; Skelly PJ; Loffing J; Shoemaker CB; Verrey F Amino-acid transport by heterodimers of 4F2hc/CD98 and members of a permease family. Nature 1998, 395, 288–291. [PubMed: 9751058]

(65). Bhutia YD; Babu E; Ramachandran S; Ganapathy V Amino acid transporters in cancer and their relevance to “glutamine addiction”: Novel targets for the design of a new class of anticancer drugs. Cancer Res. 2015, 75, 1782–1788. [PubMed: 25855379]

Author Manuscript Author Manuscript Author Manuscript Author Manuscript

(66). Matharu J; Oki J; Worthen DR; Smith QR; Crooks PA Regiospecific and conformationally restrained analogs of melphalan and DL-2-NAM-7 and their affinities for the large neutral amino acid transporter (system LAT1) of the blood-brain barrier. Bioorg. Med. Chem. Lett. 2010, 20, 3688–3691. [PubMed: 20466543]

(67). Li S; Whorton AR Identification of stereoselective transporters for S-nitroso-L-cysteine: Role of LAT1 and LAT2 in biological activity of S-nitrosothiols. J. Biol. Chem. 2005, 280, 20102–20110. [PubMed: 15769744]

(68). Friesema ECH; Docter R; Moerings EPCM; Verrey F; Krenning EP; Hennemann G; Visser TJ Thyroid hormone transport by the heterodimeric human system L-amino acid transporter. Endocrinology 2001, 142, 4339–4348. [PubMed: 11564694]

(69). Napolitano L; Galluccio M; Scalise M; Parravicini C; Eberini I; Palazzolo L; Indiveri C Novel insights into the transport mechanism of the human amino acid transporter LAT1 (SLC7A5). Probing critical residues for substrate translocation. Biochim. Biophys. Acta, Gen. Subj. 2017, 1861, 727–736. [PubMed: 28088504]

(70). Fotiadis D; Kanai Y; Palacin M The SLC3 and SLC7 families of amino acid transporters. Mol. Aspects Med. 2013, 34, 139–158. [PubMed: 23506863]

(71). Ilgu H; Jeckelmann JM; Gapsys V; Ucurum Z; de Groot BL; Fotiadis D Insights into the molecular basis for substrate binding and specificity of the wild-type L-arginine/agmatine antiporter AdiC. Proc. Natl. Acad. Sci. U. S. A. 2016, 113, 10358–10363. [PubMed: 27582465]

(72). Ilgu H; Jeckelmann JM; Colas C; Ucurum Z; Schlessinger A; Fotiadis D Effects of mutations and ligands on the thermostability of the L-arginine/agmatine antiporter AdiC and deduced insights into ligand-binding of human L-type amino acid transporters. Int. J. Mol. Sci. 2018, 19, 918.

(73). Khunweeraphong N; Nagamori S; Wiriyasermkul P; Nishinaka Y; Wongthai P; Ohgaki R; Tanaka H; Tominaga H; Sakurai H; Kanai Y Establishment of stable cell lines with high expression of heterodimers of human 4F2hc and human amino acid transporter LAT1 or LAT2 and delineation of their differential interaction with alpha-alkyl moieties. J. Pharmacol. Sci. 2012, 119, 368–380. [PubMed: 22850614]

(74). Zerangue N LAT1 Transporters Expressed in Blood—Brain Barrier Cells. U.S. Patent 7,462,459 B2, 2008.

(75). Fraga S; Serrao MP; Soares-da-Silva P The L-3,4-dihydroxyphenylalanine transporter in human and rat epithelial intestinal cells is a type 2 hetero amino acid exchanger. Eur. J. Pharmacol. 2002, 441, 127–135. [PubMed: 12063083]

(76). Forrest LR; Kramer R; Ziegler C The structural basis of secondary active transport mechanisms. Biochim. Biophys. Acta, Bioenerg. 2011, 1807, 167–188.

(77). Zamek-Gliszczynski MJ; Lee CA; Poirier A; Bentz J; Chu X; Ellens H; Ishikawa T; Jamei M; Kalvass JC; Nagar S; Pang KS; Korzekwa K; Swaan PW; Taub ME; Zhao P; Galetin A International Transporter, C. ITC recommendations for transporter kinetic parameter estimation and translational modeling of transport-mediated PK and DDIS in humans. Clin. Pharmacol. Ther. 2013, 94, 64–79. [PubMed: 23588311]

(78). Kim DK; Kanai Y; Choi HW; Tangtrongsup S; Chairoungdua A; Babu E; Tachampa K; Anzai N; Iribe Y; Endou H Characterization of the system L amino acid transporter in T24 human bladder carcinoma cells. Biochim. Biophys. Acta, Biomembr. 2002, 1565, 112–121.

(79). Meier C; Ristic Z; Klauser S; Verrey F Activation of system L heterodimeric amino acid exchangers by intracellular substrates. EMBO J. 2002, 21, 580–589. [PubMed: 11847106]

(80). Segawa H; Fukasawa Y; Miyamoto K; Takeda E; Endou H; Kanai Y Identification and functional characterization of a Na+-independent neutral amino acid transporter with broad substrate selectivity. J. Biol. Chem. 1999, 274, 19745–19751. [PubMed: 10391916]

(81). Kim CS; Cho SH; Chun HS; Lee SY; Endou H; Kanai Y; Kim DK BCH, an inhibitor of system L amino acid transporters, induces apoptosis in cancer cells. Biol. Pharm. Bull. 2008, 31, 1096–1100. [PubMed: 18520037]

(82). Procopiou PA; Ahmed M; Jeulin S; Perciaccante R Synthesis of (R)-α-benzylmethionine: A novel rearrangement during alkylation of the Seebach (R)-methionine oxazolidinone. Org. Biomol. Chem. 2003, 1, 2853–2858. [PubMed: 12968335]

Author Manuscript Author Manuscript Author Manuscript Author Manuscript

(83). Glunz PW; Rich DH Reduction of sterically hindered α,α-disubstituted amino esters. Synth. Commun. 1999, 29, 835–842.

(84). Grozinger KG; Kriwacki RW; Leonard SF; Pitner TP A novel stereoselective route to (S)-(+)-a-(fluoromethyl)histidine: alpha-halomethylation of (2R,4S)-3-benzoyl-2-(1,1-dimethylethyl)-1-methyl-4-[(N-tritylimidazol-4-yl)methyl]-1,3-imidazolidin-5-one. Synthesis and proton NMR spectroscopy. J. Org. Chem. 1993, 58, 709–713.

(85). Paju A; Kostomarova D; Matkevits K; Laos M; Pehk T; Kanger T; Lopp M 3-Alkyl-1,2-cyclopentanediones by Negishi cross-coupling of a 3-bromo-1,2-cyclopentanedione silyl enol ether with alkylzinc reagents: An approach to 2-substituted carboxylic acid γ-lactones, homocitric and lycoperdic acids. Tetrahedron 2015, 71, 9313–9320.

(86). Jackson RFW; Wishart N; Wood A; James K; Wythes MJ Preparation of enantiomerically pure protected 4-oxo α-amino acids and 3-aryl α-amino acids from serine. J. Org. Chem. 1992, 57, 3397–3404.

(87). Dexter CS; Jackson RFW; Elliott J Synthesis of enantiomerically pure β- and γ-amino acid derivatives using functionalized organozinc reagents. J. Org. Chem. 1999, 64, 7579–7585.

(88). Huo S Highly efficient, general procedure for the preparation of alkylzinc reagents from unactivated alkyl bromides and chlorides. Org. Lett. 2003, 5, 423–425. [PubMed: 12583734]

(89). Jackson RFW; Moore RJ; Dexter CS; Elliott J; Mowbray CE Concise synthesis of enantiomerically pure phenylalanine, homophenylalanine, and bishomophenylalanine derivatives using organozinc chemistry: NMR studies of amino acid-derived organozinc reagents. J. Org. Chem. 1998, 63, 7875–7884.

(90). Konda Y; Takahashi Y; Arima S; Sato N; Takeda K; Dobashi K; Baba M; Harigaya Y First total synthesis of Mer-N5075A and a diastereomeric mixture of α and β-MAPI, new HIV-1 protease inhibitors from a species of streptomyces. Tetrahedron 2001, 57, 4311–4321.

(91). Espejo VR; Rainier JD Total synthesis of kapakahine E and F. Org. Lett. 2010, 12, 2154–2157. [PubMed: 20345161]

(92). Jackson RFW; Perez-Gonzalez M Synthesis of N-(tert-butoxycarbonyl)-β-iodoalanine methyl ester: A useful building block in the synthesis of nonnatural α-amino acids via palladium catalyzed cross coupling reactions. Org. Synth. 2005, 81, 77–88.

(93). Skold N; Nielsen B; Olsen J; Han L; Olsen L; Madsen U; Kristensen JL; Pickering DS; Johansen TN Design, synthesis and in vitro pharmacology of GluK1 and GluK3 antagonists. Studies towards the design of subtype-selective antagonists through 2-carboxyethyl-phenylalanines with substituents interacting with non-conserved residues in the GluK binding sites. Bioorg. Med. Chem. 2014, 22, 5368–5377. [PubMed: 25172149]

(94). Kruppa M; Imperato G; Konig B Synthesis of chiral amino acids with metal ion chelating side chains from L-serine using Negishi cross-coupling reaction. Tetrahedron 2006, 62, 1360–1364.

(95). Manolikakes G; Schade MA; Hernandez CM; Mayr H; Knochel P Negishi cross-couplings of unsaturated halides bearing relatively acidic hydrogen atoms with organozinc reagents. Org. Lett. 2008, 10, 2765–2768. [PubMed: 18529011]

(96). Han C; Buchwald SL Negishi coupling of secondary alkylzinc halides with aryl bromides and chlorides. J. Am. Chem. Soc. 2009, 131, 7532–7533. [PubMed: 19441851]

(97). Shelby Q; Kataoka N; Mann G; Hartwig J Unusual in situ ligand modification to generate a catalyst for room temperature aromatic C-O bond formation. J. Am. Chem. Soc. 2000, 122, 10718–10719.

(98). Lundt BF; Johansen NL; Voelund A; Markussen J Removal of t-butyl and t-butoxycarbonyl protecting groups with trifluoroacetic acid. Mechanisms, byproduct formation and evaluation of scavengers. Int. J. Pept. Protein Res. 1978, 12, 258–268. [PubMed: 744685]

(99). Seebach D; Imwinkelried R; Weber T EPC (enantiomerically pure compound) syntheses with carbon-carbon bond formation via acetals and enamines. Mod. Synth. Methods 1986, 4, 125–259.

(100). Seebach D; Aebi JD; Naef R; Weber T Alpha-alkylation of amino acids without racemization. Preparation of either (S)- or (R)-α-methyldopa from (S)-alanine. Helv. Chim. Acta 1985, 68, 144–154.

(101). Garbaccio RM; Wolkenberg SE Product Subclass 10: 2-Aminoalkanoic Acid Esters (α-Amino Acid Esters) In Science of Synthesis: Category 3, Compounds with Four and Three Carbon-

Author Manuscript Author Manuscript Author Manuscript Author Manuscript

Heteroatom Bonds, Volume 20b, Three Carbon-Heteroatom Bonds: Esters and Lactones; Peroxy Acids and R(CO)OX Compounds; R(CO)X, X = S, Se, Te; Thieme: New York, 2007; Vol. 20b, pp 1131–1202.

(102). Coe DM; Perciaccante R; Procopiou PA Potassium trimethylsilanolate induced cleavage of 1,3-oxazolidin-2- and 5-ones, and application to the synthesis of (R)-salmeterol. Org. Biomol. Chem. 2003, 1, 1106–1111. [PubMed: 12926383]

(103). Karady S; Amto JS; Weinstock LM Enantioretentive alkylation of acyclic amino acids. Tetrahedron Lett. 1984, 25, 4337–4340.

(104). Cheng H; Keitz P; Jones JB Design and synthesis of a conformationally restricted cysteine protease inhibitor. J. Org. Chem. 1994, 59, 7671–7676.

(105). Sullivan DF; Woodbury RP; Rathke MW The self-condensation reaction of lithium ester enolates. Isolation of a ketene intermediate. J. Org. Chem. 1977, 42, 2038–2039.

(106). Cantor JM; Ginsberg MH CD98 at the crossroads of adaptive immunity and cancer. J. Cell Sci. 2012, 125, 1373–1382. [PubMed: 22499670]

(107). Gomes P; Soares-da-Silva P L-DOPA transport properties in an immortalised cell line of rat capillary cerebral endothelial cells, RBE 4. Brain Res. 1999, 829, 143–150. [PubMed: 10350540]

(108). Though we incubate cells with an extracellular concentration of [3H]-gabapentin of 6 nM, the intracellular concentration could be much higher due to accumulation of compound inside the cells.

(109). Akanuma SI; Yamakoshi A; Sugouchi T; Kubo Y; Hartz AMS; Bauer B; Hosoya KI Role of L-type amino acid transporter 1 at the inner blood-retinal barrier in the blood-to-retina transport of gabapentin. Mol. Pharmaceutics 2018, 15, 2327–2337.

(110). Yamamoto A; Akanuma S; Tachikawa M; Hosoya K Involvement of LAT1 and LAT2 in the high- and low-affinity transport of L-leucine in human retinal pigment epithelial cells (ARPE-19 cells). J. Pharm. Sci. 2010, 99, 2475–2482. [PubMed: 19890975]

(111). Aldrich C; Bertozzi C; Georg GI; Kiessling L; Lindsley C; Liotta D; Merz KM Jr.; Schepartz A; Wang S The ecstasy and agony of assay interference compounds. J. Med. Chem. 2017, 60, 2165–2168. [PubMed: 28244745]

Author Manuscript Author Manuscript Author Manuscript Author Manuscript

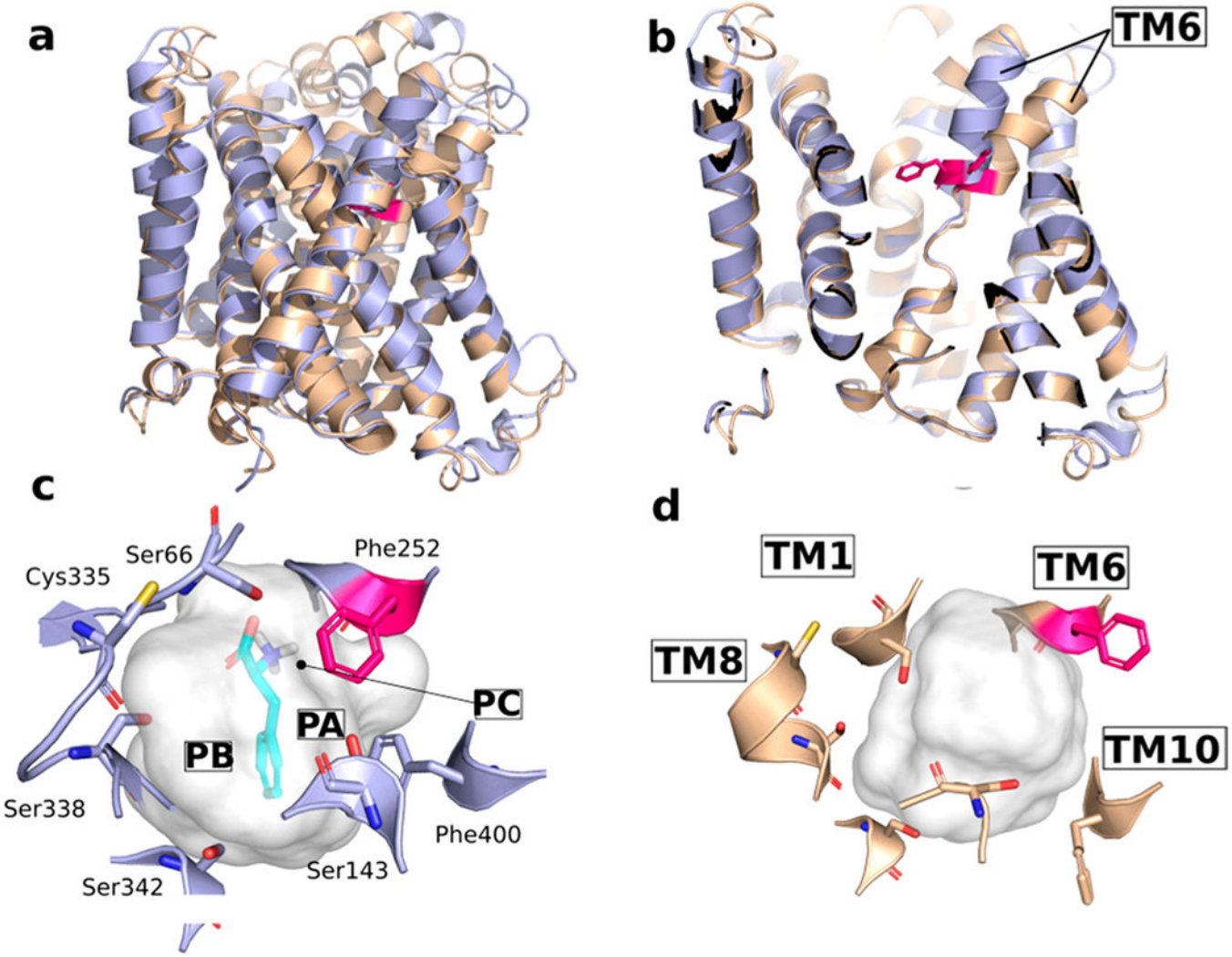

Figure 1.

Homology models of LAT1 in outward-occluded (blue) and outward-open conformations (beige). (a) The superposed models are shown in a plane perpendicular to the membrane. (b) The models are shown through a “clipped plane” perpendicular to the membrane to visualize the gate, defined by Phe252 on TM6 (pink sticks). Docking pose of phenylalanine (cyan) in the (c) occluded model and (d) open conformation. The surface of the binding site is shown in transparence, highlighting the subpockets PA and PB.

Author Manuscript Author Manuscript Author Manuscript Author Manuscript

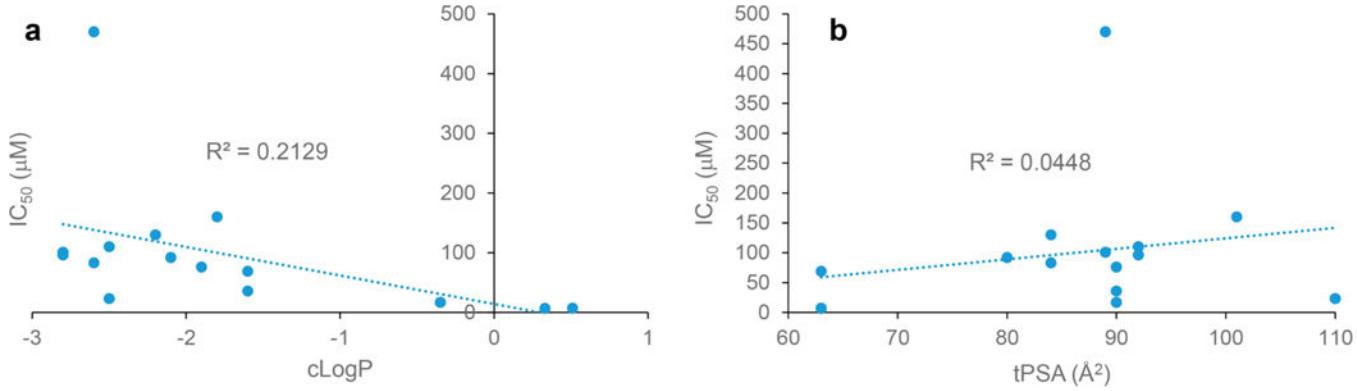

Figure 2.

Scatter plots of IC_{50} values of *meta*-substituted L-phenylalanine analogues (Table 1) vs cLogP (a) and tPSA (b), indicating poor correlation between ligand polarity and potency. Calculated properties were obtained using ChemDraw v.16.

Author Manuscript Author Manuscript Author Manuscript Author Manuscript

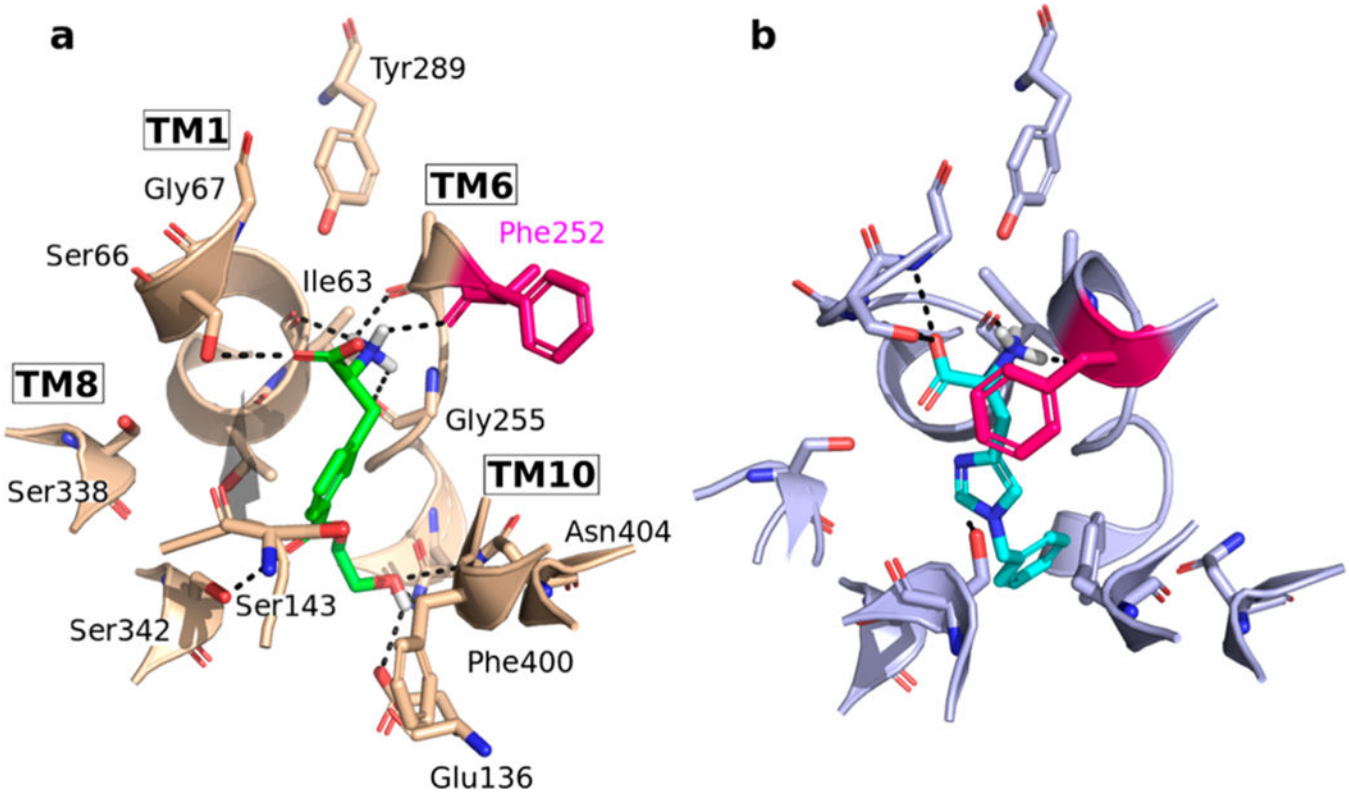

Figure 3.

Docking poses of two newly discovered substrates. (a) Compound **82**, shown in green sticks is docked in the outward-open conformation (beige). (b) Compound **59**, shown in cyan sticks, is docked in the outward-occluded conformation (light blue). While both compounds occupy PA, as predicted, compound **82** establishes additional hydrogen bonds with Glu136 and Ser342.

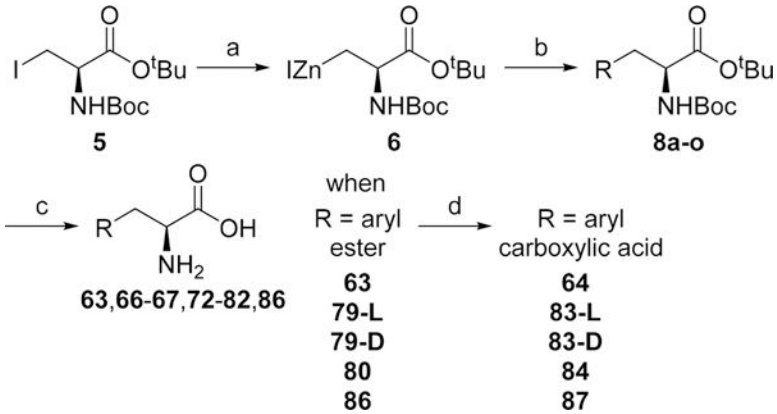

Scheme 1.

Synthesis of Compounds 63–64, 66–67, 72–84, 86, and 87[a]

[a]Reagents and conditions: (a) Zn, I_2, DMF, sonication or vigorously stirred at rt, 18 h; (b) RBr, aryl bromides **7a–7o**, $Pd_2(dba)_3$, P(*o*-tolyl)$_3$, DMF, rt, 18 h, 17–51%, flash chromatography; (c) TFA, DCM, anisole, rt, 18 h, 15–72%, preparative HPLC; (d) LiOH, water, rt, 18 h, 57–82%, preparative HPLC.

Author Manuscript Author Manuscript Author Manuscript Author Manuscript

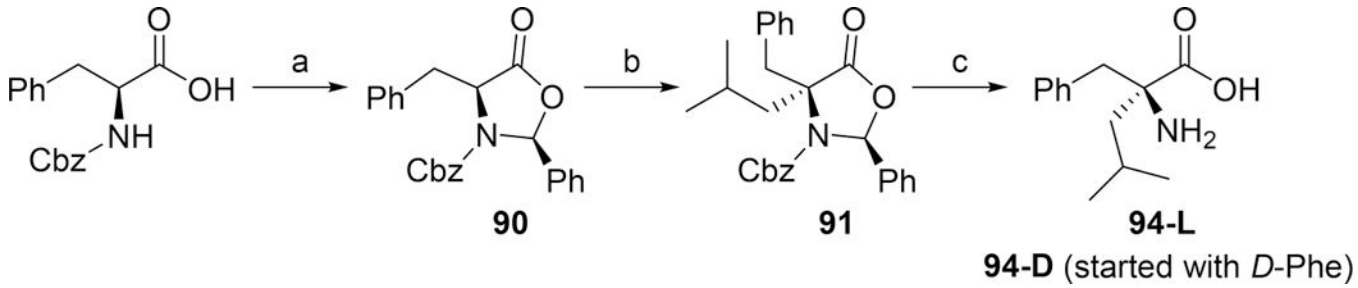

Scheme 2.

Synthesis of Compounds 94 and 94-D (Started with D-Phe)[a]

[a]Reagents and conditions: (a) $PhCH(OMe)_2$, BF_3-OEt_2, Et_2O, –78° to rt, 4 d, 44%, crystallization to give >95% single diastereomer; (b) KHMDS, isobutyl triflate, THF, –78° to rt, 18 h, 72%, flash chromatography; (c) $KOSiMe_3$, THF, 75 °C, 3 h, 55%, preparative HPLC.

Author Manuscript Author Manuscript Author Manuscript Author Manuscript

Author Manuscript Author Manuscript Author Manuscript Author Manuscript

Table 1.

Author Manuscript Author Manuscript Author Manuscript Author Manuscript

Relative Exchange Efflux Rate, Uptake Inhibition of [^{3}H]-Gabapentin, and IC_{50} Values in HEK-hLAT1 Cells for Various Natural and Non-natural, Heterocyclic, and Aromatic-Substituted Amino Acids

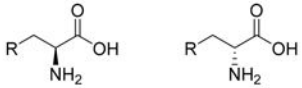

all compounds below are L isomers unless indicated otherwise

Compound[a]	R	%L-Phe Efflux[b]	% Inhibition[c]	IC_{50} (μM)[d]
50 (L-Phe)	Ph-	100	85	69 ± 29
50-D (D-Phe)	Ph-	96	74	46 ± 23
51 (L-Tyr)	*para*-HOPh-	96	68	68 ± 34
52 (L-Trp)		59	79	160 ± 87
53 (L-His)		140	92	$20\bar{}$ ± 9
54 (L-Arg)	$NH_2(NH)CNH(CH_2)_2$-	28	49	-
55 (L-Lys)	$NH_2(CH_2)_3$-	33	-2.1	-
56 (L-Asp)	HO_2C-	27	4.2	-
57 (L-Glu)	HO_2CCH_2-	27	-2.4	-
58		85	70	190 ± 25
59		81	74	170 ± 53
60		140	84	160 ± 56
61		130	98	69 ± 17
62		89	99	$10\bar{0}$ ± 53
63		56	71	95 ± 18
64		28	$3\bar{0}$	680 ± 340
110		120	32	$20\bar{0}$ ± 73
110-D		130	42	260 ± 79

Compound[a]	R	%L-Phe Efflux[b]	% Inhibition[c]	IC_{50} (μM)[d]
	R = *meta*-X-Ph, where X is			
65	Me-	140	73	-
66	CF_3-	59	87	-
67	NC-	70	67	-
68	*t*-Bu-	44	101	-
69	$PhCH_2$-	29	98	7.3 ± 3
70	Ph-	29	98	6.6 ± 3
71	HO-	96	97	130 ± 65
72	NH_2-	$10\bar{0}$	$10\bar{0}$	$10\bar{1}$ ± 35
73	$HOCH_2$-	120	99	83 ± 37
74	NH_2CH_2-	78	27	470 ± 210
75		110	85	110 ± 42
76		$10\bar{0}$	88	96 ± 32
77		96	$10\bar{0}$	92 ± 70
78		37	54	-
79		89	81	36 ± 23
79-D		41	$4\bar{0}$	150 ± 45
80		52	72	76 ± 20
81		$7\bar{0}$	99	17 ± 56
82		74	81	29 ± 10
83		56	69	130 ± 64
83-D		31	9.0	-
84		24	25	-
	R = *para*-X-Ph, where X is			
85	Me-	$10\bar{0}$	86	-
86		67	37	260 ± 90
87		$2\bar{0}$	8.9	-

Author Manuscript Author Manuscript Author Manuscript Author Manuscript

[a]Cell assay data was obtained at least in triplicate (wells) in each condition. Amino acids were either purchased (**50–62, 65, 71, 85**), synthesized as previously published (**68–70**),[56] or synthesized according to Scheme 1. All compounds above are single enantiomers of L configuration, unless indicated otherwise.

[b]Compounds were tested at 200 μM for their ability to cause efflux (fmol/min) of [^{3}H]-gabapentin from preloaded HEK-hLAT1 cells. Efflux of [^{3}H]-gabapentin was calculated at 3 min after adding test compound. %Efflux was normalized relative to L-Phe (**50**), which had an efflux rate of 2.7 ± 0.3 fmol/min, from an average of seven experiments.

[c]Compounds were tested at 200 μM for their ability to inhibit uptake of [^{3}H]-gabapentin into HEIK-hLAT1 cells. Data are presented as % inhibition relative to background signal in the absence of a test compound.

[d]For IC_{50} determinations, varying concentrations of each compound were added, from 0.1 to 500 μM. IC_{50} and standard deviation of each compound were calculated by Graphpad Prism version 5.0. %[^{3}H]-gabapentin uptake at each concentration was normalized relative to % inhibition by BCH[80,51] at 2 mM, which was set to 100% inhibition.

Author Manuscript Author Manuscript Author Manuscript Author Manuscript

Table 2.

Relative Exchange Efflux Rate, Uptake Inhibition of [^{3}H]-Gabapentin, and IC_{50} Values in HEK-hLAT1 Cells for α-Substituted Phenylalanine Derivatives

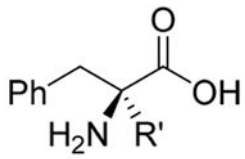

L isomers

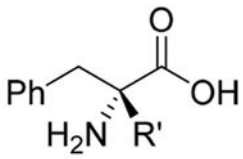

D isomers

Compound[a]	R'	%L-Phe Efflux[b]	% Inhibition[c]	IC_{50} (μM)[d]
50 (L-Phe)	H	100	85	69 ± 29
50-D (D-Phe)	H	96	74	46 ±23
92	Me-	100	-	130 ±28
92-D	Me-	100	-	810 ±350
93	$PhCH_2$ (achiral)	23	11	-
94	$(CH_3)_2CHCH_2$-	19	15	-
94-D	$(CH_3)_2CHCH_2$-	27	2.1	-
98	$CH_3S(CH_2)_2$-	56	21	240 ± 63
98-D	$CH_3S(CH_2)_2$-	27	−0.20	-
107	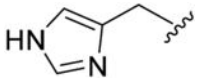	13	19	-

[a]Cell assay data was obtained at least in triplicate (wells). Amino acids were either purchased (**50, 93**), synthesized according to Scheme 2 (**92**), or as previously published (**98**,[82] **107**[83,84]). All compounds above are either single enantiomers of l configuration, or achiral (**93**), with the exception of the following compounds: **94-D** (86% ee), **98** (78% ee), **98-D** (80% ee), as determined by chiral HPLC analysis (Supporting Information).

[b]Compounds were tested at 200 μM for their ability to cause efflux (fmol/min) of [^{3}H]-gabapentin from preloaded HEK-hLAT1 cells. Efflux of [^{3}H]-gabapentin was calculated at 3 min after adding test compound. %Efflux was normalized relative to L-Phe (**50**), which had an efflux rate of 2.7 ± 0.3 fmol/min, from an average of seven experiments.

Author Manuscript Author Manuscript Author Manuscript Author Manuscript

[c]Compounds were tested at 200 μM for their ability to inhibit uptake of [^{3}H]-gabapentin into HEK-hLAT1 cells. Data are presented as % inhibition relative to background signal in the absence of a test compound.

[d]For IC_{50} determinations, varying concentrations of each compound were added, from 0.1 to 500 μM. IC_{50} and standard deviation of each compound were calculated by Graphpad Prism version 5.0. %[^{3}H]-gabapentin uptake at each concentration was normalized relative to %inhibition by BCH[80,81] at 2 mM, which was set to 100% inhibition.

Author Manuscript Author Manuscript Author Manuscript Author Manuscript

Table 3.

Relative Exchange Efflux Rate, Uptake Inhibition of [^{3}H]-Gabapentin, and IC_{50} Values in HEK-hLAT1 Cells for L and D Isomers of Endogenous LAT1 Substrates and Various Nonsubstrate Amino Acids

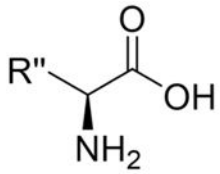

L isomers

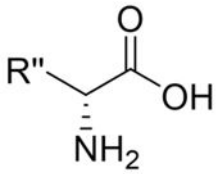

D isomers

Compound[a]	R"	%L-Phe Efflux[b]	% Inhibition[c]	IC_{50} ((μM)[d]
45 (Gly)	H (achiral)	29	33	-
46 (L-Leu)	$(CH_3)_2CHCH_2$-	120	73	85 ± 21
46-D (D-Leu)	$(CH_3)_2CHCH_2$-	100	56	220 ± 47
47 (L-Ile)	(*S*)-$CH_3CH_2(CH_3)CH$-	93	-	140 ± 27
47-D (D-Ile)	(*S*)-$CH_3CH_2(CH_3)CH$-	78	18	>3,000
48 (L-Met)	$CH_3S(CH_2)_2$-	89	-	170 ±23
48-D (D-Met)	$CH_3S(CH_2)_2$	110	56	120 ±33
49 (L-Val)	$(CH_3)_2CH$-	100	43	68 ±21
49 D (D-Val)	$(CH_3)_2CH$-	41	11	>50,000
50 (L-Phe)	$PhCH_2$-	100	85	69 ±29
50-D (D-Phe)	$PhCH_2$-	96	74	46 ±23
51 (L-Tyr)	*para*-$HOPhCH_2$-	96	68	68 ± 34

Author Manuscript Author Manuscript Author Manuscript Author Manuscript

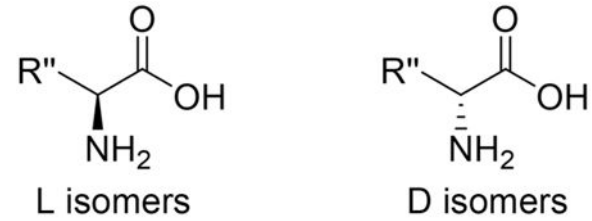

Compound[a]	R"	%L-Phe Efflux[b]	% Inhibition[c]	IC_{50} ((μM)[d]
51-D (D-Tyr)	*para*-$HOPhCH_2$-	85	35	380 ± 73
52 (L-Trp)	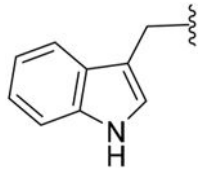	59	79	160 ± 87
52-D (D-Trp)	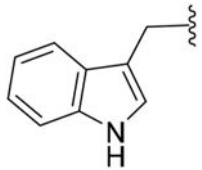	81	29	380 ± 130
53 (L-His)	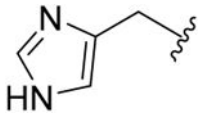	140	92	20 ± 9
53-D (D-His)	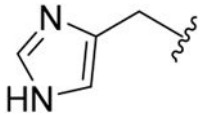	78	33	460 ± 170
54 (L-Arg)	$NH_2(NH)CNH(CH_2)_3$-	28	49	-

Author Manuscript Author Manuscript Author Manuscript Author Manuscript

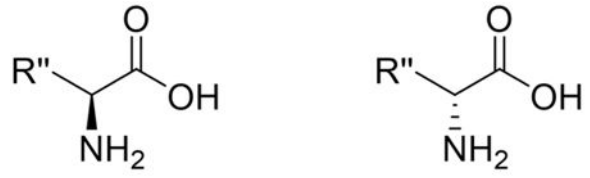

L isomers D isomers

Compound[a]	R"	%L-Phe Efflux[b]	% Inhibition[c]	IC_{50} ((μM)[d]
55 (L-Lys)	$NH_2(CH_2)_4$-	33	−2.1	-
56 (L-Asp)	HO_2CCH_2-	27	4.2	-
57 (L-Glu)	$HO_2C(CH_2)_2$-	27	−2.4	-

[a]Cell assay data was obtained at least in triplicate (wells). Amino acids were purchased from commercial vendors. All compounds above are single enantiomers of L configuration, unless indicated otherwise. Most of these amino acids (except **54–57**) were converted and tested as their HCl salts to improve water solubility.

[b]Compounds were tested at 200 *μM* for their ability to cause efflux (fmol/min) of [^{3}H]-gabapentin from preloaded HEK-hLAT1 cells. Efflux of [^{3}H]-gabapentin was calculated at 3 min after adding test compound. %Efflux was normalized relative to L-Phe (**50**), which had an efflux rate of 2.7 ± 0.3 fmol/min, from an average of seven experiments.

[c]Compounds were tested at 200 *μM* for their ability to inhibit uptake of [^{3}H]-gabapentin into HEK-hLAT1 cells. Data is presented as % inhibition relative to background signal in the absence of a test compound.

[d]For IC_{50} determinations, varying concentrations of each compound were added, from 0.1 to 500 *μM*. IC_{50} and standard deviation of each compound were calculated by Graphpad Prism version 5.0. %[^{3}H]-gabapentin uptake at each concentration was normalized relative to % inhibition by BCH[80,81] at 2 mM, which was set to 100% inhibition.